European Journal of Medicinal Chemistry 211 (2021) 113114

Contents lists available at ScienceDirect

European Journal of Medicinal Chemistry

journal homepage: http://www.elsevier.com/locate/ejmech

Research paper

Structure-based discovery of 1*H*-indole-2-carboxamide derivatives as potent ASK1 inhibitors for potential treatment of ulcerative colitis

Shaohua Hou [a, 1], Xiping Yang [c, 1], Yu Tong [a], Yuejing Yang [a], Quanwei Chen [a], Boheng Wan [a], Ran Wei [a], Yuchen Wang [a], Yanmin Zhang [a], Bo Kong [a], Jianhang Huang [a], Yadong Chen [a, b], Tao Lu [a, b, ***], Qinghua Hu [c, **], Ding Du [a, *]

[a] School of Sciences, China Pharmaceutical University, 639 Longmian Avenue, Nanjing, 211198, PR China
[b] State Key Laboratory of Natural Medicines, China Pharmaceutical University, 24 Tongjiaxiang, Nanjing, 210009, PR China
[c] School of Pharmacy, China Pharmaceutical University, 639 Longmian Avenue, Nanjing, 211198, PR China

ARTICLE INFO

Article history:
Received 26 October 2020
Received in revised form
16 December 2020
Accepted 16 December 2020
Available online 25 December 2020

Keywords:
ASK1 inhibitor
1*H*-indole-2-carboxamide derivatives
Ulcerative colitis

ABSTRACT

Apoptosis signal-regulating kinase 1 (ASK1), a member of the mitogen-activated protein kinase (MAPK) family, is implicated in many human diseases. Here, we describe the structural optimization of hit compound **7** and conduct further structure-activity relationship (SAR) studies that result in the development of compound **19** with a novel indole-2-carboxamide hinge scaffold. Compound **19** displays potent anti-ASK1 kinase activity and stronger inhibitory effect on ASK1 in AP1-HEK293 cells than previously described ASK1 inhibitor GS-4997. Besides improved *in vitro* activity, compound **19** also exhibits an appropriate *in vivo* PK profile. In a dextran sulfate sodium (DSS)-induced mouse model of ulcerative colitis (UC), compound **19** shows significant anti-UC efficacy and markedly attenuates DSS-induced body weight loss, colonic shortening, elevation in disease activity index (DAI) and inflammatory cell infiltration in colon tissues. Mechanistically, compound **19** represses the phosphorylation of ASK1-p38/JNK signaling pathways and suppresses the overexpression of inflammatory cytokines. Together, these findings suggest that ASK1 inhibitors can potentially be used as a therapeutic strategy for UC.

1. Introduction

Ulcerative colitis (UC), a major clinical type of inflammatory bowel disease (IBD), is characterized by an uncontrolled inflammatory response, mucosal inflammation and ulceration. UC usually involves a combination of severe diarrhea, abdominal pain and weight loss [1–3]. The morbidity of the UC tends to be increasing in recent years in the Middle East, South America, Asia, and much of the developing world. Moreover, UC greatly impairs the quality of life of patients and UC is also associated with an increased risk of colorectal cancer (CRC) [4,5], which has a significant global impact on public health. Although the pathogenesis of UC has not been completely revealed, immune dysregulation caused by various genetic and environmental factors has been considered as a major cause [6,7]. Emerging literature suggests that excessive pro-inflammatory cytokines play a key role in the occurrence of UC, such as TNF-α, IL-1β, IL-6, and IFN-γ [8–12]. Currently, therapeutic medications for UC include aminosalicylate, glucocorticoids, immunosuppressive agents and biologics [13]. However, severe side effects, economic burdens, limited efficacy and administration compliance of these drugs greatly limit their clinical applications [14,15]. These limitations dictate an urgent need to develop new anti-UC drugs with better therapeutic efficacy and better safety.

Apoptosis signal-regulating kinase 1 (ASK1) is a member of the mitogen-activated protein kinase (MAPK) family that activates the c-Jun *N*-terminal kinase (JNK) and p38 MAPK signaling pathways [16]. ASK1 is activated in response to various forms of cellular stress including reactive oxygen species (ROS), endoplasmic reticulum (ER) stress, bacterial and viral infections, calcium influx and inflammatory signals [17]. ASK1 has been reported to be

* Corresponding author.
** Corresponding author.
*** Corresponding author. School of Sciences, China Pharmaceutical University, 639 Longmian Avenue, Nanjing, 211198, PR China.
E-mail addresses: lutao@cpu.edu.cn (T. Lu), huqh@cpu.edu.cn (Q. Hu), ddmn9999@cpu.edu.cn (D. Du).
[1] Shaohua Hou and Xiping Yang contributed equally to this work. The manuscript was written through contributions of all authors.

https://doi.org/10.1016/j.ejmech.2020.113114
0223-5234/

involved in cell death, survival, differentiation or apoptosis [18]. Recent studies reveal that ASK1 is related to a number of human pathological conditions including inflammatory, tumorigenesis, neurodegenerative disorders, cardiovascular and metabolic disorders [19,20]. Consequently, pharmacological inhibition of ASK1 by small molecules represents a promising strategy to ameliorate these human diseases [21]. For instance, compound **1** (K811, Fig. 1) was reported to be effective in a $SOD1^{G93A}$ transgenic mouse model of amyotrophic lateral sclerosis (ALS) [22]. In addition, K811 presented a therapeutic potential for gastric cancer in *in vitro* and *in vivo* assays [23]. Compound **2** was shown to be protective in an isolated heart perfusion model of heart failure [24]. Compound **3**, a preclinical candidate compound from Gilead, demonstrated significant efficacy in several rodent models of acute and chronic kidney diseases [25]. In a rat collagen-induced arthritis (CIA) model, compound **4** could improve the joint damage in a dose-dependent manner [26]. Moreover, a novel imidazopyridine-based selective ASK1 inhibitor **5** was obtained through structure-based design and optimization [27]. The development of ASK1 small molecule inhibitors with different structural types may have a potential clinical application value. However, in recent years, the therapeutic application of ASK1 small molecule inhibitors on ASK1-related diseases progresses slowly. Only GS-4997 (**6**, selonsertib) from Gilead Sciences has been evaluated in clinical trials, but failed to reach clinical endpoints in two phase III clinical trials of nonalcoholic steatohepatitis (NASH) [28]. Considering ASK1 as an important therapeutic drug target, it is reasonable to further explore the potential benefits of ASK1 inhibition in various diseases.

ASK1 is involved in the regulation of many inflammatory responses. Specifically, markedly elevated mRNA and protein levels of ASK1 is observed in sodium fluoride (NaF)-induced mouse liver inflammatory responses [29]. MiR-23b, an endogenous short non-coding single-stranded RNA molecule, has been reported to suppress the inflammatory responses in the process of cutaneous wound healing by targeting ASK1 [30]. Atsushi and his colleagues found that ASK1 is required for LPS-induced p38 activation, resulting in the production of pro-inflammatory cytokines including IL-6, TNF-α and IL-1β [31]. Gurung et al. reported that RIF-ASK1-MAPK signaling is activated in 2,4,6-trinitrobenzene sulfonic acid (TNBS)-induced UC [32]. The Ca^{2+}/ASK1/MKK7/JNK2/cSrc signaling pathway is related to DSS-induced tight junction disruption and barrier dysfunction, which may lead to an inflammatory process and colitis [33]. Moreover, Baregamian et al. demonstrated that ASK1-JNK/p38 stress signaling and mitochondrial apoptotic cascade are activated in rat intestinal epithelial cells treated with TNF-α [34]. Hence, we focused our effort to investigate the effect of ASK1 inhibitors on UC.

Here, we report our structure-guided discovery of small molecule ASK1 inhibitors based on the 1*H*-indole-2-carboxamide derivatives. Our efforts have yielded the discovery of compound **19** as a potent and orally active small molecule inhibitor of ASK1, which exhibits good efficacy in a DSS-induced mouse model of UC, suggesting that ASK1 inhibitors may have potential therapeutic utility for the treatment of UC disease.

2. Chemistry

As presented in Schemes 1–**5**, a total of 22 target compounds were prepared. The synthesis of compounds **8**–**14**, **19**, **20**, **26** is highlighted in Scheme 1. Commercially available methyl 6-aminopicolinate reacted with hydrazine hydrate in EtOH to give 6-aminopicolinohydrazide **8-b**, which was treated with DMF-DMA to provide **8-c**. The key intermediate **8-d** was prepared by reacting **8-c** with isopropylamine in the presence of acetic acid in acetonitrile. Treatment of appropriate acids with oxalyl chloride provided acid chloride, which underwent amide formation with **8-d** to generate the target compounds in DCM.

Compound **15** was generated via the synthetic route illustrated in Scheme 2. Bromination of compound **11** with NBS followed by a Pd-catalyzed Suzuki cross-coupling reaction of **15-a** with 2-(furan-3-yl)-4,4,5,5-tetramethyl-1,3,2- dioxaborolane gave the target compound.

The preparation of compounds **16**, **17**, **21**–**24**, **27**–**29** is depicted in Scheme 3. Conversion of the appropriate acid **16-a**, **17-a**, **21-a**, **27-a** to the acid chloride followed by amide formation with intermediate **8-d** furnished **16-b**, **17-b**, **21-b**, **27-b**. Suzuki cross-coupling between the prepared bromine intermediates and appropriate aromatic borates gave the desired products.

The synthesis of compound **18** is depicted in Scheme 4. (*R*)-2-(3-(6-aminopyridin-2-yl)-4*H*-1,2,4-triazol-4-yl)propan-1-ol **18-a** was produced by a cyclization of **8-c** with (*R*)-2-aminopropan-1-ol. O-TBS protection of **18-a** and subsequent amide coupling between **18-b** and 1*H*-indole-2-carbonyl chloride gave **18-c**, which underwent O-TBS deprotection to afford the target compound **18**.

The preparation of compound **25** is shown in Scheme 5. Conversion of 2-nitrophenylhydrazine **25-a** to **25-b** was followed by Fischer Indole Synthesis to furnish **25-c**. **25-e** was obtained by reduction of **25-c** with Fe and NH_4Cl in ethanol followed by amide coupling of **25-d** with acetyl chloride in DCM. Hydrolysis of **25-e** with sodium hydroxide and amide coupling of **25-f** with **8-d** gave the desired compound **25**.

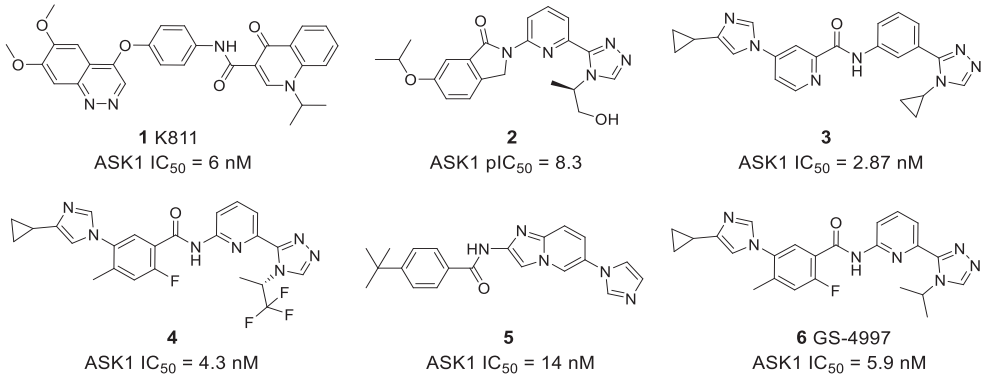

Fig. 1. Representative ASK1 small molecule inhibitors.

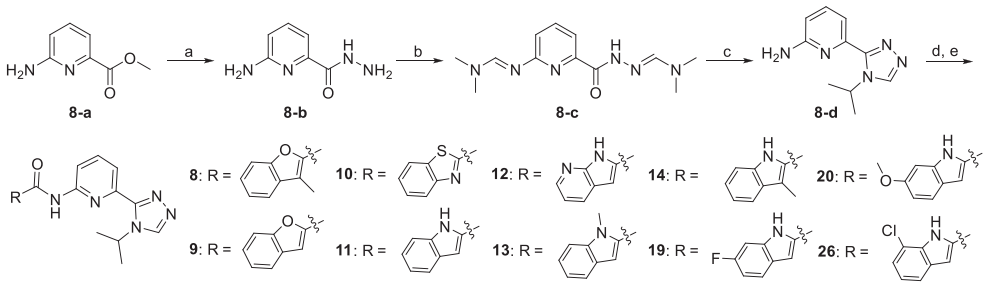

Scheme 1. *Reagents and conditions*: (a) hydrazine hydrate, EtOH, 90 °C, 12 h; (b) DMF-DMA, ref, 3 h; (c) isopropylamine, CH_3CN/CH_3COOH 5:1, 75 °C, 4 h; (d) oxalyl chloride, DMF, DCM, 0 °C to rt, 1 h; (e) pyridine, DCM, 0 °C to rt, 2 h.

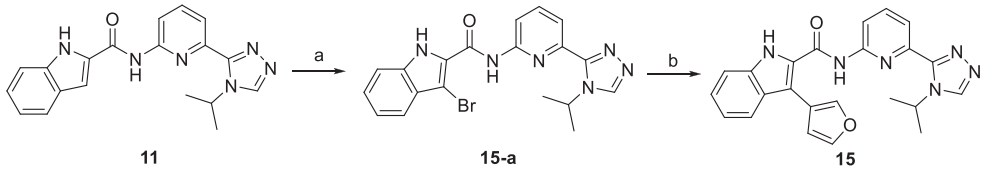

Scheme 2. *Reagents and conditions*: (a) NBS, THF, rt, 2 h; (b) $Pd(dppf)Cl_2$, K_2CO_3, 2-(furan-3-yl)-4,4,5,5-tetramethyl-1,3,2-dioxaborolane, 1,4-dioxane/H_2O 5:1, 100 °C, N_2, 6 h.

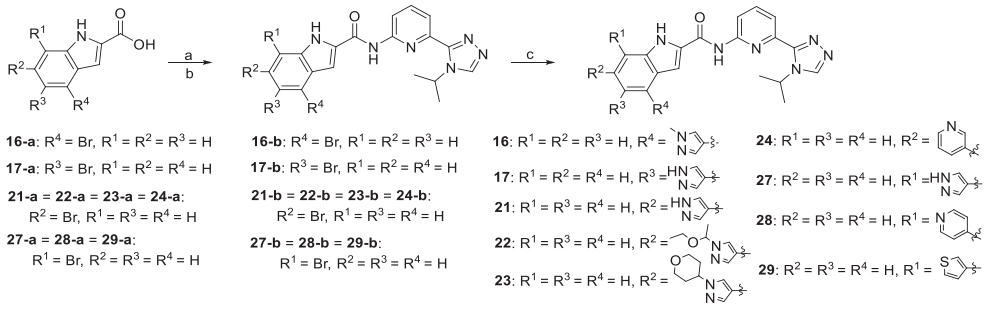

Scheme 3. *Reagents and conditions*: (a) oxalyl chloride, DMF, DCM, 0 °C to rt, 1 h; (b) pyridine, DCM, 0 °C to rt, 2 h; (c) $Pd(dppf)Cl_2$, K_3PO_4, corresponding pinacol ester, 1,4-dioxane/H_2O 5:1, 110 °C, 3 h.

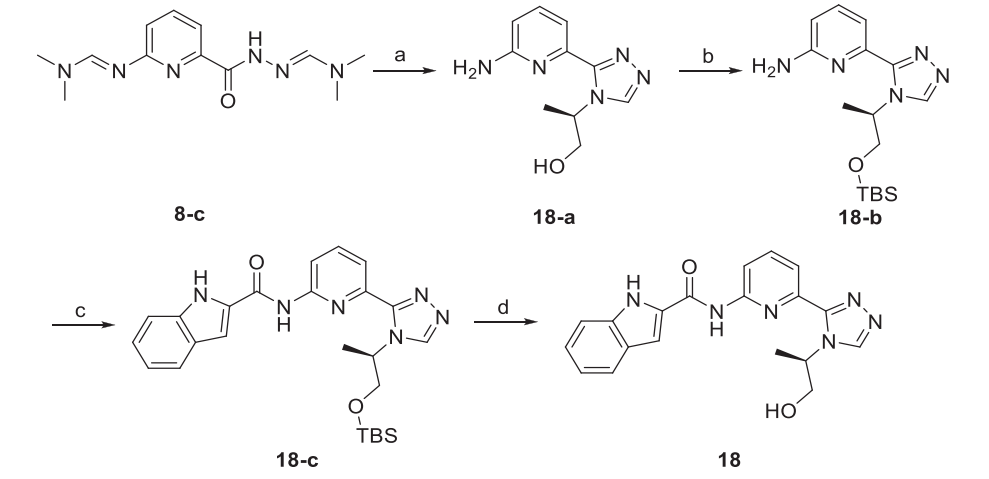

Scheme 4. *Reagents and conditions*: (a) isopropylamine, CH_3CN/CH_3COOH 5:1, 75 °C, 4 h; (b) tert-butyldimethylsilyl chloride, DIPEA, DME, rt, 2 h; (c) 1*H*-indole-2-carbonyl chloride, pyridine, DCM, 0 °C to rt, 2 h; (d) TBAF, THF, rt, 2 h.

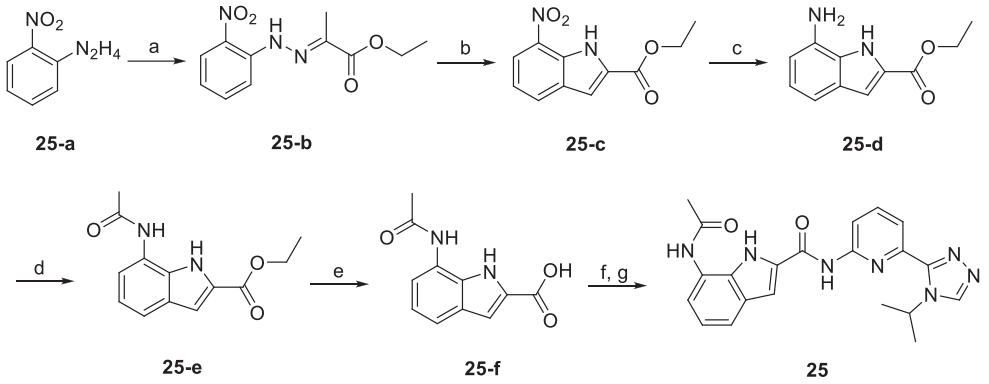

Scheme 5. *Reagents and conditions*: (a) ethyl pyruvate, EtOH, rt, 12 h; (b) polyphosphoric acid, 80 °C, 3 h; (c) Fe, NH_4Cl, EtOH/H_2O (6:1), 80 °C, 4 h; (d) acetyl chloride, DIPEA, DCM, rt, 3 h; (e) NaOH, THF/H_2O 5:1, rt, 3 h; (f) oxalyl chloride, DMF, DCM, 0 °C to rt, 1 h; (g) pyridine, DCM, 0 °C to rt, 2 h.

3. Results and discussion

3.1. Structure-based design strategy

In our previous work, hit compound **7** (Fig. 3) (ASK1 IC_{50} = 16700 ± 2130 nM) was identified from our in-house compound library. To improve its kinase potency, first, publicly available crystallographic data and some pharmacophore models were studied to better understand the molecular interactions between ligands and ASK1 protein [35–40]. We found that almost all ASK1 inhibitors interact with the hinge region in ASK1 active site by forming crucial hydrogen bond interaction with Val757. Typically, the binding modes of compounds **5** and **6** are as drawn in Fig. 2. Cocrystal structure 3VW6 reveals that compound **5** interacts with hinge region through the hydrogen bond donor and receptor motif of 2-*N*-acylimidazopyridine core, and the imidazole ring of compound **5** also interacts with Lys709 deeper in the kinase active site. The *t*-butyl phenyl group is sandwiched between Arg705 and Lys769, pointing to the solvent-exposed region and the phenyl ring stacking over Gly759. Moreover, docking analysis of **6** showed that the amide carbonyl core of **6** forms a key hydrogen bond with the backbone NH of Val757 acting as a single-point hinge binder. Meanwhile, the triazole interacts with Lys709 through an important hydrogen bond interaction, and a cyclopropyl-imidazole group reaches the solvent exposed region around the protein [24,27,41].

Then, based on hit compound **7**, we further developed potent ASK1 small molecule inhibitors with a novel hinge-binder scaffold. As outlined in Fig. 3, we initially preserved the core amine and triazole ring of **6** to maintain the key hydrogen bonds with Val757 and Lys709, replacing the benzene group with 3-methylbenzofuran from hit **7** affording compound **8**. Meanwhile, various fused aromatic heterocycles, including benzofuran ring and benzothiazole ring, were incorporated into compounds **9**–**10**. Moreover, compounds **11**–**12** with an indole ring and azaindole, respectively, were designed with the aim of forming an additional interaction with Val757 in the hinge region (Table 1).

3.2. Inhibitory activity against ASK1

Compounds **8**–**12** were prepared from key intermediate **8-d** (Scheme 1) and submitted for kinase potency studies. The results of the kinase inhibition assay are listed in Table 1. As expected, compound **8** showed a remarkable increase in ASK1 potency compared to hit **7**, with ASK1 IC_{50} of 1106 ± 24 nM. Unexpectedly, benzofuran derivative **9** had significantly enhanced potency in ASK1 kinase assay compared to 3-methylbenzofuran **8**. We speculated that the introduction of methyl is detrimental to the benzofuran ring to remain coplanar with the rest of the core, which is pivotal for suitable binding of compound **8** to the ATP-binging site [24,41,42]. Moreover, benzothiazole analogue **10** exhibited a greater than 3-fold loss in potency in comparison with compound **9**. Interestingly, an indole ring replacement (**11**) yielded a more than 3-fold increase in potency compared to initial compound **9**. To better understand the results, a docking model derived from PDB 5VIO was used to predict the binding modes of compounds **9** and **11** in the ASK1 active site. As seen from Fig. 4, docking studies confirmed two key hydrogen-bond interactions, that is, the carbonyl group of core amine forming a H bond with backbone NH of Val757 and N1 triazole nitrogen participating in a H bond with catalytic Lys709. Nevertheless, the indole NH of compound **11**, distinct from compound **9**, had an additional H bond with the backbone carbonyl of Val757 in the hinge region, resulting in a dramatic increase of potency observed in compound **11**. However, azaindole **12** showed 3-fold reduced ASK1 potency than **11** and an equipotent effect to compound **9**, indicating that an electron-deficient pyridine ring is not tolerated well in this area. Therefore, we focused further optimization and modification on indole derivative **11**.

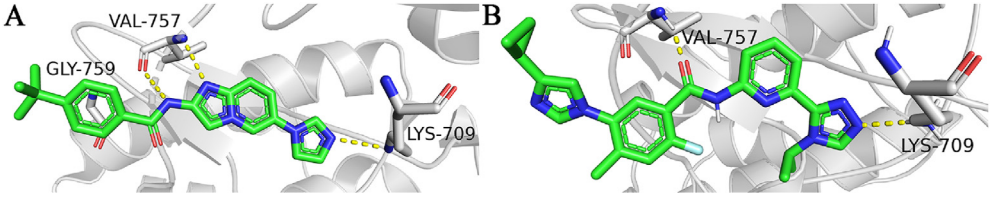

Fig. 2. (A) Cocrystal of compound 5 in ASK1 (PDB code: 3VW6). (B) Compound 6 modeled into ASK1 (PDB code: 5VIO). The ligands and important residues are shown in stick form. The hydrogen bonds are depicted as yellow dashed lines. (For interpretation of the references to color in this figure legend, the reader is referred to the Web version of this article.)

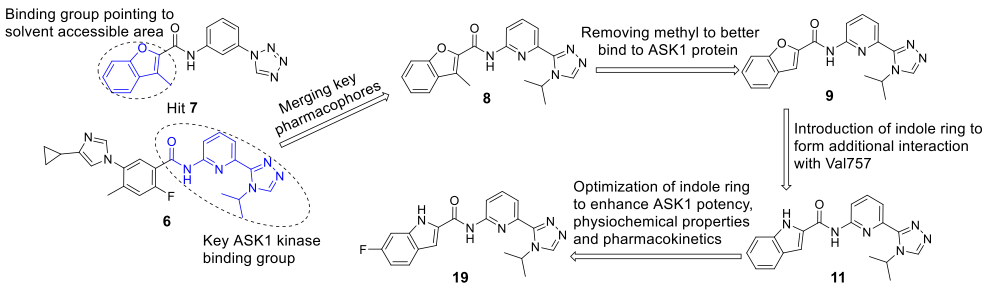

Fig. 3. Structure-based design and optimization of 1*H*-indole-2-carboxamide derivatives as ASK1 inhibitors.

Table 1
Inhibitory activity of compounds 7–12 against ASK1.

Cpds	Structure	ASK1 IC_{50}(nM)[a]
7	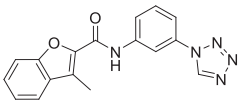	16700 ± 2130
8	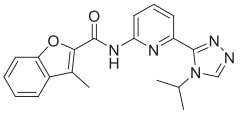	1106 ± 24
9	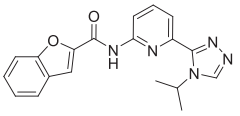	151.6 ± 11
10	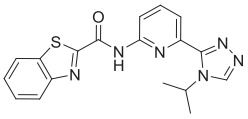	506 ± 12
11	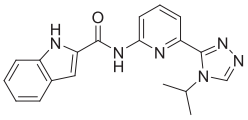	41.4 ± 2.17
12	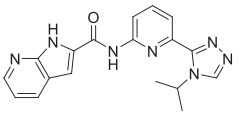	125.1 ± 12.10

[a] IC_{50} values are the mean ± SD from two independent experiments.

Starting from the promising compound **11**, we expanded the chemical space of ASK1 inhibitors for further SAR exploration and identified a potent ASK1 inhibitor (compound **19**) with an acceptable ADME profile (Fig. 3). 1*H*-indole-2-carboxamide analogues containing substituents at the N1 nitrogen atom and 3-, 4-, 5-, 6-, 7-positions of the 1*H*-indole ring were designed and prepared. The *in vitro* ASK1 potency of these compounds is shown in Table 2–**3**. First, 1-methyl-1*H*-indole derivative **13** showed a dramatically decreased ASK1 kinase inhibition compared to 1*H*-indole derivative **11** as expected (see Table 2), confirming the importance of the H bond between Val757 and 1*H*-indole. Similar to compound **8**, installation of a methyl (**14**) or furan appendage (**15**) to the 3-position of indole also resulted in decreased activity compared to the unsubstituted indole **11**. Specifically, the ASK1 potency of furan analogue **15** is inferior to that of methyl analogue **14**, perhaps due to the steric bulk of the furan ring being greater than that of methyl and thus more likely to disturb the planarity of molecule. We also explored the 4-position and 5-position of the indole ring by introduction of *N*-methylpyrazole (**16**) and pyrazole (**17**) respectively, in which both showed slightly improved kinase activity. We speculated that the 4-position and 5-position of the indole ring point to the solvent-accessible area and have no significant impact on ASK1 potency. Moreover, replacing isopropyl (**11**) with (*R*)-1-hydroxypropan-2-yl (**18**) resulted in comparable ASK1 kinase activity.

Inspired by the overlay of compounds **11** and **6** in the ASK1 active site (Fig. 4B), we further explored the 6-position and 7-position of the indole ring. As shown in Table 3, installation of an electron-withdrawing group F (**19**) at the 6-position of the unsubstituted indole slightly improved ASK1 kinase potency, and the electron-donating group OCH_3-substituted derivative (**20**) exhibited slightly diminished potency. Moreover, placing a pyrazole moiety at the 6-position (**21**) restored the binding affinity relative to parent indole **11**. We further explored the SAR of the solvent-accessible region by substituting the pyrazole group with 1-ethoxyethyl (**22**) and tetrahydropyran (**23**) and replacing pyrazole with pyridine (**24**). Compounds **22**–**24** all showed decreased molecular activity, likely attributed to larger aromatic heterocyclic substituents not well tolerated in this area.

Next, the introduction of an acetamido group to the 7-position of the indole ring yielded compound **25**, leading to a significant decrease in ASK1 inhibition. The addition of an electron-withdrawing group Cl (**26**) to the 7-position also resulted in a

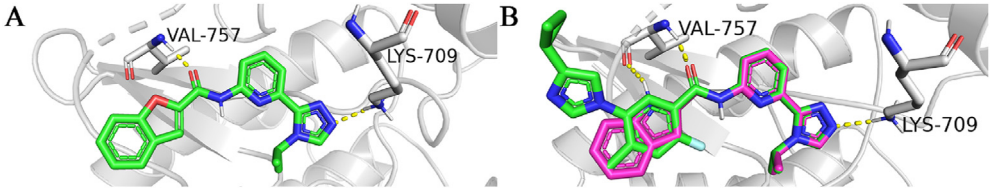

Fig. 4. (A) Compound 9 modeled into ASK1 (PDB code: 5VIO). (B) Compound 11 overlaid 6 modeled into ASK1 (PDB code: 5VIO). The ligands and important residues are shown in stick form. The hydrogen bonds are depicted as yellow dashed lines. (For interpretation of the references to color in this figure legend, the reader is referred to the Web version of this article.)

Table 2
Inhibitory activity of compounds 13–18 against ASK1.

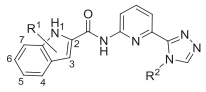

Cpds	Pos[a]	R^1	R^2	$ASKIC_{50}$ (nM)[b]	Cpds	Posa	R^1	R^2	$ASKIC_{50}$ (nM)[b]
13	1-			743 ± 48	**16**	4-			19.6 ± 3.05
14	3-			88.2 ± 6.18	**17**	5-			31.6 ± 1.61
15	3-			142.8 ± 6.55	**18**	–	H		65.5 ± 3.61

[a] Substituted position of R^1 on the indole ring.
[b] IC_{50} values are the mean ± SD from two independent experiments.

Table 3
Inhibitory activity of compounds **19**–**29** against ASK1.

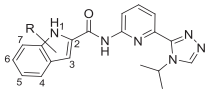

Cpds	Pos[a]	R	$ASKIC_{50}$ (nM)[b]	Cpds	Pos[a]	R	$ASKIC_{50}$ (nM)[b]
19	6-		32.8 ± 1.88	**25**	7-		240.1 ± 8.05
20	6-		54.3 ± 4.87	**26**	7-		89.6 ± 4.16
21	6-		37.5 ± 2.79	**27**	7-		38.9 ± 2.26
22	6-		91.1 ± 1.77	**28**	7-		23.1 ± 2.19
23	6-		73.7 ± 4.62	**29**	7-		153.3 ± 7.65
24	6-		68.5 ± 9.55				

[a] Substituted position of R on the indole ring.
[b] IC_{50} values are the mean ± SD from two independent experiments.

Table 4
AP1-HEK293 cell activity of select compounds.

Cpds	Inhibition rate (%) at 10 μM[b]	Cpds	Inhibition rate (%) at 10 μM[b]
6	76.67 ± 1.13	**19**	95.59 ± 0.24
9	25.33 ± 3.10	**20**	95.93 ± 1.10
11	56.46 ± 0.29	**21**	94.39 ± 0.25
12	32.54 ± 1.91	**22**	94.04 ± 1.36
14	92.48 ± 0.88	**23**	64.63 ± 1.45
16	72.88 ± 0.14	**24**	95.66 ± 1.29
17	89.55 ± 2.61	**26**	90.84 ± 0.02
18	61.26 ± 0.44	**27**	59.86 ± 1.88

[b] Values are the mean ± SD from three independent experiments.

Table 5
Permeability assay of compounds **6** and **19** in MDRI-MDCKII cells[a].

Cpds	P-gp inhibitor	P_{app} ($\times 10^{-6}$ cm/s) (N = 2)		Efflux ratio	P-gp substrate[c]
		A→B	B→A		
6	without	11.22	26.47	2.4	Yes
	with CsA[b]	34.49	25.02	0.7	
19	without	21.12	15.63	0.7	No
	with CsA	36.62	26.05	0.7	

[a] Cells that overexpress P-gp.
[b] A known P-gp inhibitor ciclosporin A.
[c] Efflux ratio (ER) ≥ 2 and the ER decreases to < 50% of the ER in the absence of inhibitor.

slightly decreased affinity to ASK1 when compared with compound **11**. Furthermore, the five-membered aromatic heterocyclic pyrazole-substituted analogue **27** and six-membered aromatic heterocyclic pyridine-substituted analogue **28** showed a slightly increased inhibition against ASK1. However, the thiophene ring (**29**) is not well tolerated in this area, with a diminished ASK1 potency (IC_{50} = 153.3 ± 7.65 nM).

3.3. AP1-HEK293 cell activity

To evaluate the drug likeness and cell membrane permeability of these compounds, we analyzed the cellular potency of select compounds in AP1-HEK293 cells that contain a firefly luciferase gene under the control of AP1-responsive elements stably integrated into HEK293 cells. Stress-induced activation of ASK1 leads to phosphorylation and activation of JNKs via MMK4/7. Activated JNKs then translocate to the nucleus where they phosphorylate and activate transcription factors such as c-Jun, which binds to the activator protein-1 (AP1) response element and induces AP1-driven luciferase reporter activity that can be reduced by the treatment of ASK1 inhibitors.

A total of 15 compounds were selected for AP1-HEK293 cell assay. As illustrated in Table 4, the majority of these compounds showed good inhibition of reporter activity in AP1-HEK293 cells at 10 μM, with inhibition rate typically greater than 50% except benzofuran **9** and azaindole **12** that were less potent with inhibition rate of 25.33 ± 3.10% and 32.54 ± 1.91%, respectively. This is consistent with their *in vitro* ASK1 kinase potency. In addition, eight 1*H*-indole-2-carboxamide derivatives had better AP1-HEK293 cellular activity than **6**, with inhibition rate of compounds **19**, **20**, and **24** all greater than 95%. These results indicated that this series of compounds might have appropriate physicochemical properties supporting our rational design for further evaluation.

To better understand why compound **6** showed a stronger ASK1 kinase inhibition (IC_{50} = 5.9 nM, Fig. 1) compared to compound **19** (IC_{50} = 32.8 ± 1.88 nM, Table 3) while being less active in the AP1-HEK293 cellular assay, we compared their membrane permeability in MDRI-MDCKII cell-based assay. As shown in Table 5, compound **19** ($P_{app(A\rightarrow B)}$ = 21.12 × 10^{-6} cm/s) had a better cell membrane permeability than compound **6** ($P_{app(A\rightarrow B)}$ = 11.22 × 10^{-6} cm/s). Moreover, unlike compound **19**, compound **6** was identified to be a P-gp substrate, which is subject to removal from the cells by an ATP-dependent efflux pump. That could explain its lesser activity in the AP1-HEK293 cell activity assay.

3.4. Pharmacokinetic properties

With the aim of investigating the pharmacokinetic (PK) profile of these 1*H*-indole-2-carboxamides and based on the favorable *in vitro* kinase and AP1-HEK293 cell activity, compound **19** was subsequently evaluated in a rat PK study. As shown in Table 6, compound **19** had low *in vivo* clearance (CL = 1.38 L/h/kg) and moderate half-life ($T_{1/2}$ = 1.45 h) after iv administration at a dose of 1 mg/kg. Moreover, following oral administration at 10 mg/kg, compound **19** showed high oral exposure (AUC_{last} = 4517 h*ng/mL), 62.2% oral bioavailability and acceptable terminal half-life ($T_{1/2}$ = 2.31 h). These data fully justified to assess the efficacy of compound **19** in *in vivo* murine animal models. Judging from published data (Table 7), compound **6** also exhibited a favorable PK profile in rats. Upon a single iv dose (1 mg/kg), it showed low clearance rate (CL = 0.11 L/h/kg), modest volume of distribution (V_{ss} = 0.55 L/kg) and long half-life ($T_{1/2}$ = 5.07 h), and upon oral administration at an oral dose of 5 mg/kg, compound **6** had a good oral bioavailability (75%).

3.5. Compound 19 improved DSS-induced UC

Due to the favorable PK profile and good *in vitro* potency, compounds **19** and **6** was further evaluated in a DSS-induced mouse UC model. In this model, ICR mice were given 3% DSS drinking water from day 1 to day 7. Weight loss, diarrhea, and rectal bleeding were observed from day 3, indicating that the UC model was successfully established. Compounds **19** and **6** were administered orally at a dose of 25 mg/kg per day from day 1 to day 7.

As demonstrated in Fig. 5A, the body weights of all experimental mice increased slightly in the first two days. However, compared with the vehicle-treated normal control group, the body weights of DSS-treated model group mice decreased significantly by −9.6%, unlike a continued increase seen in the control group. Oral administration of compound **19** at a dose of 25 mg/kg to the DSS-treated experimental mice induced a significant recovery of body weight loss, with an increase of +11.2%. Although compound **6** treatment also exhibited a certain therapeutic effect, it failed to prevent body weight loss. As shown in Fig. 5B, the disease activity index (DAI) score of the control group remained nearly unchanged throughout the experiment. Treatment with DSS induced a 2.83 unit increase in DAI score. In contrast to the DSS model group, the DAI score of the compound **19** group showed about a 2 unit decrease, with the compound **6** (i.e., GS-4997) group showing a 0.83 unit decrease. These results suggested that compounds **19** and **6** could improve symptoms of the UC mice, in which compound **19** exhibited a stronger alleviation than compound **6**.

Given colon shortening is also an obvious symptom in DSS-induced UC mice, measurement of the colon length in all the experimental mice showed that compound **19** significantly prevented colon shortening induced by DSS. As shown in Fig. 5C and **D**, the colon length of the normal control group was 9.63 cm, the percentage of colon shortening of DSS model group was 26.7% (colon length: 7.05 cm). In contrast, the percentage of colon shortening of compound **19** group was 14.8% (colon length: 8.20 cm), while the percentage of colon shortening of compound **6** group was 23.4% (colon length: 7.37 cm). To further confirm the therapeutic effect of compound **19**, we performed a histopathological analysis of colon tissues. As shown in Fig. 5E, DSS treatment induced a severe colonic tissue damage and infiltration of inflammatory cells. Consistent with previous results, compound **19** significantly attenuated these pathological changes of colon tissues. Compound **6** also produced a certain protective effect. Taken together, compound **19** showed a significant protective effect in the DSS-induced colitis mouse model.

Table 6
Pharmacokinetic (PK) profile of compound **19** in rats[a].

Parameters[b]	iv (1 mg/kg)	Parameters[b]	po (10 mg/kg)
CL(L/h/kg)	1.38 ± 0.106	T_{max}(h)	2.00 ± 0.17
V_{ss}(L/kg)	2.82 ± 0.225	C_{max}(ng/mL)	676 ± 101
AUC_{last}(h*ng/mL)	713 ± 51.5	AUC_{last}(h*ng/mL)	4517 ± 1042
AUC_{INF}(h*ng/mL)	727 ± 54.7	AUC_{INF}(h*ng/mL)	4521 ± 1043
$T_{1/2}$(h)	1.45 ± 0.0885	$T_{1/2}$(h)	2.31 ± 0.112
MRT_{INF}(h)	2.04 ± 0.109	F(%)	62.2 ± 14.4

[a] Male Sprague Dawley rats iv at 1 mg/kg and the dosing solution was prepared in 10% DMAC + 10% (30% Solutol HS 15 in water) + 80% Saline, po at 10 mg/kg and the dosing suspension was prepared in 0.5% CMC and 0.5% Tween 80 in water.
[b] PK parameters are the mean ± SD from three independent experimental rats.

Table 7
Pharmacokinetic (PK) profile of compound **6** in rats[a].

Cpd	CL (L/h/kg), iv	V_{ss}(L/kg), iv	$T_{1/2}$(h), iv	F(%)
6	0.11	0.55	5.07	75

[a] Referenced to https://www.cortellis.com/drugdiscovery, iv dose 1 mg/kg and po dose 5 mg/kg.

3.6. Compound 19 blocked ASK1-p38/JNK signaling pathways in DSS-induced mouse colon tissues

To better understand the molecular mechanism underlying the anti-inflammatory activity of compounds **19** and **6**, we performed Western blotting to investigate the inhibitory effect of compounds **19** and **6** on ASK1-p38/JNK signaling pathways involved in the regulation of various inflammatory responses. As shown in Fig. 6A and B, DSS treatment resulted in an upregulation of phosphorylation of ASK1, MKK3/6, MKK4/7, and downstream p38 and JNK in colon tissues when compared with the control group. However, abnormally elevated phosphorylated proteins of ASK1-p38/JNK signaling pathways were effectively reversed by compound **19**, with compound **6** showing weaker effects than that of compound **19**. These data suggested that ASK1-p38/JNK signaling is important for compounds **19**- and **6**-mediated protection in DSS-induced acute colitis mice.

3.7. Reduction of inflammatory cytokine levels by compound 19 in DSS-induced mouse colon tissues

Increasing literature highlights an abnormal upregulation of pro-inflammatory cytokines, such as IL-1β, IL-6 and TNF-α, is important in the pathogenesis of UC. To further define the anti-inflammatory mechanism of compounds **19** and **6**, enzyme-linked immunosorbent assay (ELISA) was conducted to examine the expression levels of these inflammatory cytokines in colon tissues. As shown in Fig. 6C, the significantly enhanced levels of IL-1β, IL-6 and TNF-α in DSS-treated mice were decreased by compound **19**.

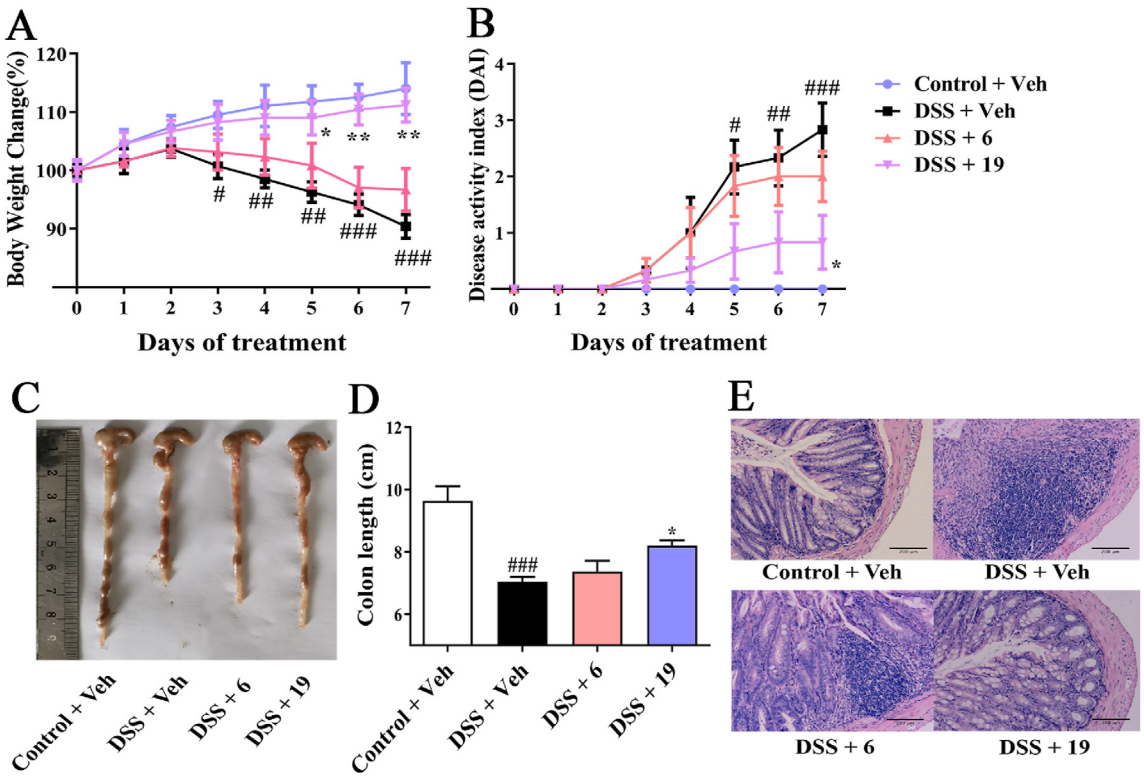

Fig. 5. Effect of compounds **19** and **6** in DSS-induced UC mice. Mice were given 3% DSS drinking water ad libitum to induce colitis. Control mice were fed with distilled water only. In addition to DSS, compounds **19** and **6**, dissolved in CMC-Na aqueous solution, were orally administered to compound **19** and compound **6** group mice, respectively. Meanwhile, CMC-Na aqueous solution were orally administered to the control group and DSS model group mice. (A) The body weight changes of each group during the experiment (n = 5–6 per group). (B) DAI scores of each group during the experiment (n = 5–6 per group). (C) Representative images of mouse colon from each group. Scale bar, 200 μm. (D) Colon length of each group (n = 4–6 per group). (E) Representative H&E staining images of the colon tissues from each group. Data are expressed as mean ± SEM. Compared with the control group: $^{\#}$ P < 0.05, $^{\#\#}$ P < 0.01, $^{\#\#\#}$ P < 0.001; Compared with the DSS + Veh group: * P < 0.05, ** P < 0.01, *** P < 0.001.

Compound **6** was also helpful but with a weaker effect. These results showed that compounds **19** and **6** could attenuated DSS-induced UC via inhibition of pro-inflammatory cytokines, including IL-1β, IL-6 and TNF-α.

4. Conclusion

In this paper, starting from our previously identified hit compound **7** containing a 3-methylbenzofuran-2-carbonyl fragment, we designed and synthesized several compounds consisting of various fused aromatic heterocycles. Interestingly, indole **11** showed a 3-fold more potent ASK1 kinase inhibitory activity than benzofuran **9**. Besides the known hydrogen bond between carbonyl of **11** and Val757, the docking study identified an additional H bond between indole NH of **11** and Val757. Subsequent structure-based optimization of compound **11** led to the discovery of compound **19** with potent anti-ASK1 kinase activity, stronger AP1-HEK293 cell inhibitory activity than compound **6**, and excellent *in vivo* PK properties.

Studies showed that the ASK1 signaling pathway is activated in the development and occurrence of UC [32], and the cellular function of ASK1 is related to inflammatory responses [43]. For these reasons, compounds **19** and **6** were subjected to the research on UC. In the DSS-induced mouse model of UC, oral administration of compound **19** could ameliorate the inflammatory symptoms of UC mice caused by DSS administration. Body weights of the compound **19** group mice are generally close to that of the control group and the DAI score of the compound **19** group also exhibited an evident decline compared to the DSS model group. Notably, colon shortening of UC mice was significantly improved by compound **19** treatment. Furthermore, histopathological examination showed that compound **19** remarkably relieved the colon tissue damage induced by DSS treatment. Compound **6** also showed a moderate protective effect in these tests. Mechanistic studies revealed that compounds **19** and **6** suppressed ASK1-MKK3/6-p38 and ASK1-MKK4/7-JNK signaling activation and reduced the up-regulated pro-inflammatory cytokines (IL-1β, TNF-α, IL-6) in the colon tissues of DSS-exposed UC mice. Compound **6** produced weaker anti-UC effect compared to compound **19**, which agrees with its relatively lower activity in the AP1-HEK293 cell-based assay. The better anti-UC effect of compound **19** could be due to its higher membrane permeability and a lack of susceptibility to the efflux through the ATP-dependent efflux pump, so that compound **19** may exert stronger therapeutic effect in the colon tissues.

In conclusion, we have discovered a series of potent ASK1 small molecule inhibitors with a novel 1*H*-indole-2-carboxamide hinge scaffold. The most promising compound **19** demonstrated significant therapeutic effects on DSS-induced UC as an ASK1 small molecule inhibitor with an anti-inflammatory action. Altogether, this research unfolds the possibility of developing orally available ASK1 inhibitors as therapeutic agents for the treatment of UC.

5. Experimental

5.1. Chemistry

All reagents and solvents are commercially available and were purchased as reagent grade and used without further purification.

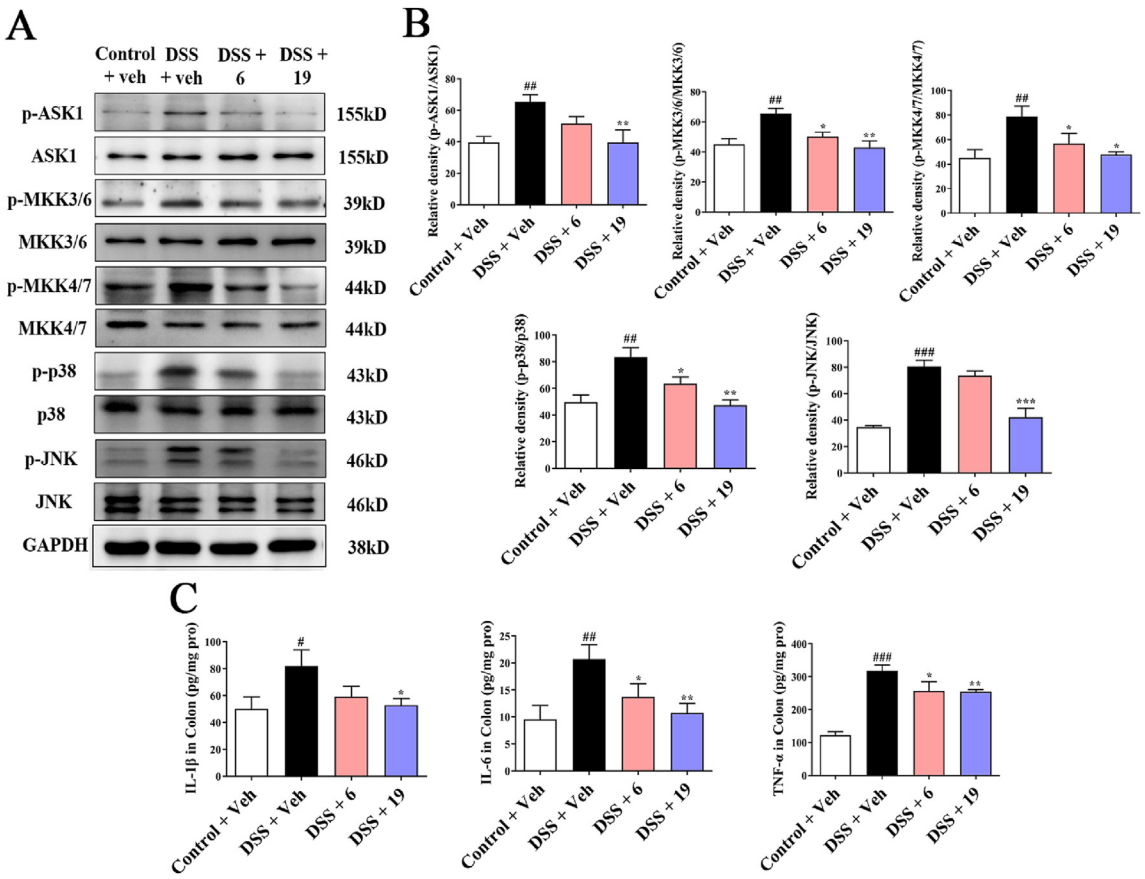

Fig. 6. Inhibitory effect of compounds **19** and **6** on activated ASK1-p38/JNK signaling and up-regulated inflammatory cytokines in colon tissues of DSS-induced UC mice. (A) Western blot analysis of the protein levels of ASK1-MKK3/6-p38 and ASK1-MKK4/7-JNK signaling pathways as well as corresponding phosphorylated proteins. GAPDH was used as the loading control protein. (B) Quantitative analysis of the ratios of phosphorylated proteins normalized to their unphosphorylated form. (C) The levels of inflammatory cytokines IL-1β, IL-6, TNF-α were detected using ELISA kits. Data are expressed as mean ± SEM (n = 5–6 per group). Compared with the control group: # P < 0.05, ## P < 0.01, ### P < 0.001; Compared with the DSS + Veh group: * P < 0.05, ** P < 0.01, *** P < 0.001.

^{1}H NMR spectra were obtained with Bruker AV-300 or Bruker AV-400. The abbreviations s, d, t, q, dd and m signify singlet, doublet, triplet, quartet, doublet of doublets and multiplet, respectively. ^{13}C NMR spectra were obtained with Bruker AV-300 or Bruker AV-400. Low-Resolution Mass Spectrometry analyses were conducted on Agilent 1100 LC/MSD mass spectrometer (Agilent, USA). High-Resolution Mass Spectrometry analyses were conducted on a Q-Tof micro spectrometer (Micromass Company). Melting points were determined with a X-4 digital-display melting-point apparatus (Beijing Tech Instrument Co., Ltd.). All reactions were monitored by thin-layer chromatography (TLC) on silica gel plates (GF254) and spots were visualized with UV light. Flash column chromatography was performed over silica gel using a mixture of ethyl acetate (EA), petroleum ether (PE), dichloromethane (DCM) and MeOH. The purity of the final compounds was assessed by high-pressure liquid chromatography (HPLC) and determined to be ≥ 95% pure.

5.1.1. *N-(6-(4-isopropyl-4H-1,2,4-triazol-3-yl)pyridin-2-yl)-3-methylbenzofuran-2-carboxamide (8)*

Step A: To a solution of methyl 6-aminopicolinate **8-a** (5.00 g, 33.0 mmol) in EtOH (10 mL) was added hydrazine hydrate (4.85 g, 99.0 mmol, 3.0 eq), the mixture was stirred at 90 °C for 12 h in pressure tube, the reaction was monitored by TLC. Upon completion, the reaction mixture was cooled to rt. The precipitate formed in the mixture was collected by filtration, washed with EA and then dried in vacuo to give 6-aminopicolinohydrazide (**8-b**) as a white solid (4.50 g, 29.3 mmol, yield: 89%). ^{1}H NMR (400 MHz, DMSO-d_6) δ 9.14 (s, 1H), 7.51 (t, J = 8.4 Hz, 1H), 7.11 (d, J = 7.2 Hz, 1H), 6.60 (d, J = 7.2 Hz, 1H), 6.07 (s, 2H), 4.47 (s, 2H). MS (ESI) [M + H]$^+$: 153.1.

Step B: A mixture of **8-b** (4.50 g, 29.0 mmol) in DMF-DMA was heated under reflux for 3 h, the reaction was monitored by TLC. Upon completion, the reaction mixture was cooled to rt and then concentrated under reduced pressure. The residue was taken up in EA (100 mL) and heated at 50 °C for 30 min. After being cooled to rt, the solid was collected by filtration and dried in vacuo to give (*E*)-*N*'-(6-(2-((*E*)-(dimethylamino)methylene)hydrazine-1-carbonyl) pyridin-2-yl)-*N*,*N*-dim ethylformimidamide (**8-c**) (5.00 g, 19.1 mmol, yield: 66%) as a white solid. ^{1}H NMR (400 MHz, DMSO-d_6) δ 10.69 (s, 1H), 8.86 (s, 1H), 8.06 (s, 1H), 7.68 (t, J = 7.7 Hz, 1H), 7.48 (d, J = 6.8 Hz, 1H), 6.91 (d, J = 8.0 Hz, 1H), 3.14 (s, 3H), 3.02 (s, 3H), 2.88 (s, 6H). MS (ESI) [M + H]$^+$: 263.2.

Step C: To a solution of compound **8-c** (5.00 g, 19.0 mmol) in a mixture of CH_3CN/AcOH (30 mL, 5:1) was added isopropylamine (5.60 g, 95.0 mmol, 5.0 eq). The resulting mixture was heated at 75 °C for 4 h, the reaction was monitored by TLC. Upon completion, the reaction mixture was cooled to rt, and the solvent was removed under reduced pressure. The residue was dissolved in water (100 mL) and 2 M NaOH was added to a pH of 8.0. The water solvent was extracted with EA (100 mL x 3). The combined organic layers were dried over anhydrous Na_2SO_4, filtered, and concentrated under reduced pressure. The resulting residue was chromatographed over silica gel (3–10% MeOH in DCM) to give 6-(4-isopropyl-4*H*-1,2,4-triazol-3-yl)pyridin-2-amine (**8-d**) (2.52 g, 12.3 mmol, yield:

65%) as a white solid. ^{1}H NMR (300 MHz, DMSO-d_6) δ 8.78 (s, 1H), 7.52 (t, J = 7.8 Hz, 1H), 7.16 (d, J = 7.4 Hz, 1H), 6.52 (d, J = 8.3 Hz, 1H), 6.17 (s, 2H), 5.62–5.45 (m, 1H), 1.43 (d, J = 6.7 Hz, 6H). MS (ESI) [M + H]$^+$: 204.1.

Step D: To a 0 °C cooled solution of 3-methylbenzofuran-2-carboxylic acid (100 mg, 0.57 mmol) and DMF (2 d) in DCM (10 mL) was added oxalyl chloride (108 mg, 0.85 mmol, 1.5 eq), the mixture was stirred at 0 °C for 10 min and then rt for 1 h. The resulting mixture was concentrated under reduced pressure to give 3-methylbenzofuran-2-carbonyl chloride as a white solid, which was used for further reaction without purification. To a 0 °C cooled solution of **8-d** (116 mg, 0.57 mmol) and pyridine (68 mg, 0.86 mmol, 1.5 eq) in DCM (10 mL) was added the prepared 3-methylbenzofuran-2-carbonyl chloride, the mixture was stirred at 0 °C for 10 min and then rt for 2 h, the reaction was monitored by TLC. Upon completion, the resulting mixture was concentrated under reduced pressure, the residue was dissolved in water (100 mL) and extracted with EA (100 mL x 3). The combined organic layers were dried over anhydrous Na_2SO_4, filtered, and concentrated under reduced pressure. The resulting residue was chromatographed over silica gel (3–15% MeOH in DCM) to give *N*-(6-(4-isopropyl-4*H*-1,2,4-triazol-3-yl)pyridin-2-yl)-3-methylbenzofuran-2-carboxamide (**8**) (100 mg, 0.28 mmol, yield: 49%) as a white solid. mp 175–177 °C. ^{1}H NMR (300 MHz, DMSO-d_6) δ 10.55 (s, 1H), 8.89 (s, 1H), 8.17 (d, J = 8.1 Hz, 1H), 8.03 (t, J = 9.0 Hz, 1H), 7.89 (d, J = 7.5 Hz, 1H),7.82 (d, J = 7.8 Hz, 1H), 7.71 (d, J = 8.1 Hz, 1H), 7.54 (t, J = 7.6 Hz, 1H), 7.39 (t, J = 7.4 Hz, 1H), 2.62 (s, 3H), 5.82–5.65 (m, 1H), 1.47 (d, J = 6.5 Hz, 6H). ^{13}C NMR (100 MHz, DMSO-d_6) δ 158.86, 153.42, 151.18, 150.40, 146.76, 143.74, 142.81, 139.98, 129.54, 128.31, 123.99, 123.95, 121.84, 119.92, 115.74, 112.46, 48.29, 23.75, 9.46. HRMS-EI m/z [M + H]$^+$ calcd for $C_{20}H_{20}N_5O_2^+$: 362.1612, found: 362.1615. HPLC analysis: retention time = 6.835 min; 98.45%.

***N*-(6-(4-isopropyl-4*H*-1,2,4-triazol-3-yl)pyridin-2-yl)benzofuran-2-carboxamide (9)** Compound **9** was prepared from benzofuran-2-carboxylic acid (100 mg, 0.37 mmol) and key intermediate **8-d** (75 mg, 0.37 mmol) according to a similar procedure described for the synthesis of compound **8** (step D). White solid, 77 mg, yield: 60%. mp 224–226 °C. ^{1}H NMR (400 MHz, DMSO-d_6) δ 10.93 (s, 1H), 8.90 (s, 1H), 8.17 (dd, J = 8.3, 0.7 Hz, 1H), 8.05 (t, J = 8.0 Hz, 1H), 7.96 (d, J = 0.8 Hz, 1H), 7.91–7.84 (m, 2H), 7.77 (dd, J = 8.4, 0.6 Hz, 1H), 7.56–7.51 (m, 1H), 7.42–7.36 (m, 1H), 5.77–5.68 (m, 1H), 1.47 (d, J = 6.7 Hz, 6H). ^{13}C NMR (100 MHz, DMSO-d_6) δ 157.71, 155.10, 151.30, 150.42, 148.50, 146.75, 143.71, 140.02, 127.97, 127.47, 124.44, 123.59, 120.02, 115.92, 112.57, 112.33, 48.29, 23.72. HRMS-EI m/z [M + H]$^+$ calcd for $C_{19}H_{18}N_5O_2^+$: 348.1455, found: 348.1459. HPLC analysis: retention time = 5.020 min, 99.25%.

***N*-(6-(4-isopropyl-4*H*-1,2,4-triazol-3-yl)pyridin-2-yl)benzo[*d*]thiazole-2-carboxamide (10)** Compound **10** was prepared from benzo[*d*]thiazole-2-carboxylic acid (75 mg, 0.42 mmol) and key intermediate **8-d** (85 mg, 0.42 mmol) according to a similar procedure described for the synthesis of compound **8** (step D). White solid, 96 mg, yield: 63%. mp 263–266 °C. ^{1}H NMR (400 MHz, DMSO-d_6) δ 11.20 (s, 1H), 8.91 (s, 1H), 8.29 (dd, J = 12.2, 8.1 Hz, 2H), 8.17 (d, J = 8.1 Hz, 1H), 8.09 (t, J = 7.9 Hz, 1H), 7.96 (d, J = 7.5 Hz, 1H), 7.72–7.63 (m, 2H), 5.75–5.65 (m, 1H), 1.49 (d, J = 6.7 Hz, 6H). ^{13}C NMR (100 MHz, DMSO-d_6) δ 164.25, 159.08, 153.00, 150.49, 150.27, 146.91, 143.86, 140.23, 137.01, 127.90, 124.91, 123.67, 120.47, 115.96, 48.31, 23.79. HRMS-EI m/z [M + H]$^+$ calcd for $C_{18}H_{17}N_6OS^+$: 365.1179, found: 365.1179. HPLC analysis: retention time = 6.790 min, 97.88%.

***N*-(6-(4-isopropyl-4*H*-1,2,4-triazol-3-yl)pyridin-2-yl)-1*H*-indole-2-carboxamide (11)** Compound **11** was prepared from 1*H*-indole-2-carboxylic acid (55 mg, 0.34 mmol) and key intermediate **8-d** (70 mg, 0.34 mmol) according to a similar procedure described for the synthesis of compound **8** (step D). White solid, 58 mg, yield: 50%. mp 259–262 °C. ^{1}H NMR (300 MHz, DMSO-d_6) δ 11.89 (s, 1H), 10.67 (s, 1H), 8.90 (s, 1H), 8.23 (d, J = 8.2 Hz, 1H), 8.04 (t, J = 8.0 Hz, 1H), 7.86 (d, J = 7.5 Hz, 1H), 7.71 (d, J = 8.0 Hz, 1H), 7.60–7.55 (m, 1H), 7.50 (d, J = 8.2 Hz, 1H), 7.26 (t, J = 7.2 Hz, 1H), 7.10 (t, J = 7.4 Hz, 1H), 5.76–5.66 (m, 1H), 1.48 (d, J = 6.7 Hz, 6H). ^{13}C NMR (100 MHz, DMSO-d_6) δ 160.64, 151.80, 150.49, 146.70, 143.64, 139.92, 137.63, 131.19, 127.34, 124.70, 122.43, 120.56, 119.59, 115.66, 112.97, 106.12, 48.32, 23.70. HRMS-EI m/z [M + H]$^+$ calcd for $C_{19}H_{19}N_6O^+$: 347.1615, found: 347.1615. HPLC analysis: retention time = 4.238 min, 99.56%.

***N*-(6-(4-isopropyl-4*H*-1,2,4-triazol-3-yl)pyridin-2-yl)-1*H*-pyrrolo[2,3-*b*]pyridine-2-carboxamide (12)** Compound **12** was prepared from 1*H*-pyrrolo[2,3-*b*]pyridine-2-carboxylic acid (64 mg, 0.39 mmol) and key intermediate **8-d** (80 mg, 0.39 mmol) according to a similar procedure described for the synthesis of compound **8** (step D). White solid, 60 mg, yield: 45%. mp 279–282 °C. ^{1}H NMR (300 MHz, DMSO-d_6) δ 12.47 (s, 1H), 10.68 (s, 1H), 8.88 (s, 1H), 8.41 (dd, J = 4.6, 1.6 Hz, 1H), 8.24 (dd, J = 9.0, 3.0 Hz, 1H), 8.16 (dd, J = 9.0, 1.6 Hz, 1H), 8.05 (t, J = 8.0 Hz, 1H), 7.86(dd, J = 8.0, 1.4 Hz, 1H), 7.51 (s, 1H), 7.18 (q, J = 4.6 Hz, 1H), 5.75–5.62 (m, 1H), 1.47 (d, J = 9.0 Hz, 6H). ^{13}C NMR (100 MHz, DMSO-d_6) δ 160.22, 151.66, 150.47, 149.21, 146.72, 143.65, 140.00, 131.66, 131.05, 119.80, 119.60, 117.23, 115.64, 105.27, 48.36, 23.70. HRMS-EI m/z [M + H]$^+$ calcd for $C_{18}H_{18}N_7O^+$: 348.1567, found: 348.1570. HPLC analysis: retention time = 3.817 min, 95.21%.

***N*-(6-(4-isopropyl-4*H*-1,2,4-triazol-3-yl)pyridin-2-yl)-1-methyl-1*H*-indole-2-carboxamide (13)** Compound **13** was prepared from 1-methyl-1*H*-indole-2-carboxylic acid (52 mg, 0.30 mmol) and key intermediate **8-d** (60 mg, 0.30 mmol) according to a similar procedure described for the synthesis of compound **8** (step D). White solid, 53 mg, yield: 49%. mp 229–231 °C. ^{1}H NMR (400 MHz, DMSO-d_6) δ 10.80 (s, 1H), 8.88 (s, 1H), 8.18 (d, J = 8.2 Hz, 1H), 8.03 (t, J = 7.9 Hz, 1H), 7.88 (d, J = 7.5 Hz, 1H), 7.73 (d, J = 7.9 Hz, 1H), 7.61 (d, J = 8.4 Hz, 1H), 7.42 (s, 1H), 7.35 (t, J = 7.6 Hz, 1H), 7.16 (t, J = 7.4 Hz, 1H), 5.84–5.68 (m, 1H), 4.04 (s, 3H), 1.45 (d, J = 6.6 Hz, 6H). ^{13}C NMR (100 MHz, DMSO-d_6) δ 161.52, 151.75, 150.39, 146.72, 143.69, 139.87, 139.44, 131.81, 125.85, 124.83, 122.45, 120.92, 119.53, 115.52, 111.14, 107.49, 48.33, 31.97, 23.71. HRMS-EI m/z [M + H]$^+$ calcd for $C_{20}H_{21}N_6O^+$: 361.1771, found: 361.1776. HPLC analysis: retention time = 5.442 min, 98.65%.

***N*-(6-(4-isopropyl-4*H*-1,2,4-triazol-3-yl)pyridin-2-yl)-3-methyl-1*H*-indole-2-carboxamide (14)** Compound **14** was prepared from 3-methyl-1*H*-indole-2-carboxylic acid (87 mg, 0.49 mmol) and key intermediate **8-d** (100 mg, 0.49 mmol) according to a similar procedure described for the synthesis of compound **8** (step D). White solid, 127 mg, yield: 72%. mp 269–271 °C. ^{1}H NMR (300 MHz, DMSO-d_6) δ 11.65 (s, 1H), 10.24 (s, 1H), 8.90 (s, 1H), 8.26 (d, J = 8.2 Hz, 1H), 8.04 (t, J = 8.0 Hz, 1H), 7.86 (d, J = 7.5 Hz, 1H), 7.69 (d, J = 8.0 Hz, 1H), 7.47 (d, J = 8.2 Hz, 1H), 7.28 (t, J = 7.4 Hz, 1H), 7.10 (t, J = 7.4 Hz, 1H), 5.71–5.57 (m, 1H), 2.61 (s, 3H), 1.47 (d, J = 6.7 Hz, 6H). ^{13}C NMR (100 MHz, DMSO-d_6) δ 161.46, 151.77, 150.41, 146.65, 143.67, 140.06, 136.28, 128.42, 127.42, 125.02, 120.52, 119.90, 119.44, 116.82, 114.89, 112.61, 48.46, 23.67, 10.36. HRMS-EI m/z [M + H]$^+$ calcd for $C_{20}H_{21}N_6O^+$: 361.1771, found: 361.1770. HPLC analysis: retention time = 5.460 min, 98.34%.

6-fluoro-*N*-(6-(4-isopropyl-4*H*-1,2,4-triazol-3-yl)pyridin-2-yl)-1*H*-indole-2-carboxamide (19) Compound **19** was prepared from 6-fluoro-1*H*-indole-2-carboxylic acid (176 mg, 0.98 mmol) and key intermediate **8-d** (200 mg, 0.98 mmol) according to a similar procedure described for the synthesis of compound **8** (step D). White solid, 292 mg, yield: 82%. mp 249–252 °C. ^{1}H NMR (300 MHz, DMSO-d_6) δ 11.95 (s, 1H), 10.72 (s, 1H), 8.88 (s, 1H), 8.21 (d, J = 8.3 Hz, 1H), 8.03 (t, J = 7.9 Hz, 1H), 7.85 (d, J = 7.6 Hz, 1H), 7.78–7.69 (m, 1H), 7.59 (s, 1H), 7.20 (d, J = 9.9 Hz, 1H), 6.97 (t,

J = 9.3 Hz, 1H), 5.78−5.60 (m, 1H), 1.47 (d, J = 6.6 Hz, 6H). ^{13}C NMR (100 MHz, DMSO-d_6) δ 160.39, 151.74, 150.54, 146.69, 143.58, 140.18, 139.90, 131.99, 124.25, 123.99, 119.67, 115.65, 109.97, 106.24, 98.53, 48.30, 23.65. HRMS-EI m/z [M + H]$^+$ calcd for $C_{20}H_{21}N_6O^+$: 365.1521, found: 365.1520. HPLC analysis: retention time = 4.366 min, 99.54%.

***N*-(6-(4-isopropyl-4*H*-1,2,4-triazol-3-yl)pyridin-2-yl)-6-methoxy-1*H*-indole-2-carboxamide (20)** Compound **20** was prepared from 6-methoxy-1*H*-indole-2-carboxylic acid (71 mg, 0.37 mmol) and key intermediate **8-d** (75 mg, 0.37 mmol) according to a similar procedure described for the synthesis of **8** (step D). White solid, 97 mg, yield: 70%. mp 242−245 °C. ^{1}H NMR (300 MHz, DMSO-d_6) δ 11.70 (s, 1H), 10.56 (s, 1H), 8.88 (s, 1H), 8.23 (d, J = 8.3 Hz, 1H), 8.02 (t, J = 7.9 Hz, 1H), 7.84 (d, J = 7.5 Hz, 1H), 7.58 (d, J = 8.7 Hz, 1H), 7.52(s, 1H), 6.93 (s, 1H), 6.75 (d, J = 8.7 Hz, 1H), 5.78−5.62 (m, 1H), 3.80 (s, 3H), 1.47 (d, J = 6.5 Hz, 6H). ^{13}C NMR (100 MHz, DMSO-d_6) δ 160.67, 158.23, 152.00, 150.63, 146.69, 143.57, 139.79, 138.81, 130.08, 123.27, 121.74, 119.46, 115.56, 112.15, 106.69, 94.57, 55.54, 48.38, 23.64. HRMS-EI m/z [M + H]$^+$ calcd for $C_{20}H_{21}N_6O_2^+$: 377.1721, found: 377.1720. HPLC analysis: retention time = 4.210 min, 99.04%.

7-chloro-*N*-(6-(4-isopropyl-4*H*-1,2,4-triazol-3-yl)pyridin-2-yl)-1*H*-indole-2-carboxamide (26) Compound **26** was prepared from 7-chloro-1*H*-indole-2-carboxylic acid (92 mg, 0.47 mmol) and key intermediate **8-d** (95 mg, 0.47 mmol) according to a similar procedure described for the synthesis of compound **8** (step D). White solid, 120 mg, yield: 67%, mp 208−211 °C. ^{1}H NMR (300 MHz, DMSO-d_6) δ 12.06 (s, 1H), 10.85 (s, 1H), 8.90 (s, 1H), 8.26 (dd, J = 6.3, 0.3 Hz, 1H), 8.06 (t, J = 8.7 Hz, 1H), 7.84 (dd, J = 7.6, 0.6 Hz, 1H), 7.68 (d, J = 6.0 Hz, 1H), 7.55 (d, J = 2.1 Hz, 1H), 7.37 (dd, J = 5.7, 0.6 Hz, 1H), 7.12 (t, J = 7.8 Hz, 1H), 5.63−5.49 (m, 1H), 1.48 (d, J = 5.1 Hz, 6H). ^{13}C NMR (100 MHz, DMSO-d_6) δ 159.92, 151.83, 150.68, 146.72, 143.52, 139.96, 134.71, 132.87, 129.08, 124.34, 121.59, 121.38, 119.98, 117.20, 115.73, 108.54, 48.38, 23.63. HRMS-EI m/z [M + H]$^+$ calcd for $C_{19}H_{18}ClN_6O^+$: 381.1225, found: 381.1225. HPLC analysis: retention time = 5.617 min, 95.52%.

3-(furan-3-yl)-*N*-(6-(4-isopropyl-4*H*-1,2,4-triazol-3-yl)pyridin-2-yl)-1*H*-indole-2-carboxamide (15) Step A: To a solution of compound **11** (200 mg, 0.57 mmol) in THF was added NBS (102 mg, 0.57 mmol, 1.0 eq), and the mixture was stirred for 2 h at rt, the reaction was monitored by TLC. Upon completion, the reaction solution was concentrated under reduced pressure. The residue was partitioned between saturated aqueous Na_2SO_3 (50 mL) and EA (50 mL). The organic layer was separated and washed with brine (50 mL), dried over Na_2SO_4, filtered, and concentrated under reduced pressure. The resulting residue was chromatographed over silica gel (3−5% MtOH in DCM) to give 3-bromo-*N*-(6-(4-isopropyl-4*H*-1,2,4-triazol-3-yl)pyridin-2-yl)-1*H*-indole-2- carboxamide (**15-a**) (198 mg, 0.46 mmol, yield: 82%) as a yellow solid. ^{1}H NMR (300 MHz, DMSO-d_6) δ 11.95 (s, 1H), 10.74 (s, 1H), 8.89 (s, 1H), 8.22 (dd, J = 8.1, 0.6 Hz, 1H), 8.04 (t, J = 8.1 Hz, 1H), 7.85 (dd, J = 7.5, 0.6 Hz, 1H), 7.70 (d, J = 5.1 Hz, 1H), 7.49 (dd, J = 8.1, 0.3 Hz, 1H), 7.25−7.10 (m, 1H), 7.08−6.78 (m, 1H), 5.73−5.53 (m, 1H), 1.47 (d, J = 9.6 Hz, 6H). MS (ESI) [M + H]$^+$: 425.1.

Step B: A mixture of **15-a** (100 mg, 0.23 mmol), Pd(dppf)Cl_2 (17 mg, 0.023 mmol, 0.1 eq), K_2CO_3 (64 mg, 0.46 mmol, 2.0 eq), 2-(furan-3-yl)-4,4,5,5-tetramethyl-1,3,2-dioxaborolane (67 mg, 0.35 mmol, 1.5 eq) in 1,4-dioxane/H_2O 5:1 (10 mL, 2 mL) was heated at 100 °C for 6 h in nitrogen atmosphere, the reaction was monitored by TLC. Upon completion, the mixture was allowed to cool to rt, filtered, the filtrate was diluted with water (50 mL) and the water solvent was extracted with EA (50 mL x 3). The combined organic layers were dried over anhydrous Na_2SO_4, filtered, and concentrated under reduced pressure. The resulting residue was chromatographed over silica gel (3−8% MtOH in DCM) to give 3-(furan-3-yl)-*N*-(6-(4-isopropyl-4*H*-1,2,4-triazol -3-yl)pyridin-2-yl)-1*H*-indole-2-carboxamide (**15**) (54 mg, 0.13 mmol, yield: 57%) as a white solid. mp 223−225 °C. ^{1}H NMR (300 MHz, DMSO-d_6) δ 12.10 (s, 1H), 9.56 (s, 1H), 8.88 (s, 1H), 8.31 (d, J = 8.0 Hz, 1H), 8.18 (s, 1H), 8.04 (t, J = 8.0 Hz, 1H), 7.94 (t, J = 1.6 Hz, 1H), 7.90 (d, J = 7.5 Hz, 1H), 7.58 (d, J = 8.1 Hz, 1H), 7.53 (d, J = 8.3 Hz, 1H), 7.32 (t, J = 7.3 Hz, 1H), 7.14 (t, J = 7.5 Hz, 1H), 6.89−6.83 (m, 1H), 5.43−5.32 (m, 1H), 1.43 (d, J = 6.7 Hz, 6H). ^{13}C NMR (100 MHz, DMSO-d_6) δ 160.52, 151.11, 150.03, 146.68, 144.58, 143.83, 142.08, 140.26, 136.51, 127.55, 127.39, 125.22, 121.02, 120.94, 119.47, 117.72, 114.44, 113.02, 112.86, 110.13, 48.63, 23.56. HRMS-EI m/z [M + H]$^+$calcd for $C_{23}H_{21}N_6O_2^+$: 413.1721, found: 413.1722. HPLC analysis: retention time = 3.917 min, 96.84%.

***N*-(6-(4-isopropyl-4*H*-1,2,4-triazol-3-yl)pyridin-2-yl)-4-(1-methyl-1*H*-pyrazol-4-yl)-1*H*-indole-2-carboxamide (16).** Step A: Compound **16-b** was prepared from 4-bromo-1*H*-indole-2- carboxylic acid **16-a** (177 mg, 0.74 mmol) and key intermediate **8-d** (150 mg, 0.74 mmol) according to a similar procedure described for the synthesis of compound **8** (step D). Yellow solid, 235 mg, yield: 75%. ^{1}H NMR (300 MHz, DMSO-d_6) δ: 11.95 (s, 1H), 10.74 (s, 1H), 8.89 (s, 1H), 8.22 (dd, J = 8.1, 0.6 Hz, 1H), 8.04 (t, J = 8.1 Hz, 1H), 7.85 (dd, J = 7.5, 0.6 Hz, 1H), 7.56 (s, 1H), 7.49 (dd, J = 8.1, 0.3 Hz, 1H), 7.32−7.21 (m, 1H), 7.08−6.88 (m, 1H), 5.73−5.57 (m, 1H), 1.47 (d, J = 9.6 Hz, 6H). MS (ESI) [M + H]$^+$: 425.1.

Step B: A mixture solution of **16-b** (100 mg, 0.24 mmol), Pd(dppf)Cl_2 (18 mg, 0.024 mmol, 0.1 eq), K_3PO_4 (102 mg, 0.48 mmol, 2.0 eq), 1-methyl-4-(4,4,5,5-tetramethyl-1,3,2-dioxaborolan- 2-yl)-1*H*-pyrazole (75 mg, 0.36 mmol, 1.5 eq) in 1,4-dioxane/H_2O (10 mL, 2 mL) was heated at 110 °C for 3 h, the reaction was monitored by TLC. Upon completion, the mixture was allowed to cool to rt, filtered, the filtrate was diluted with water (50 mL) and the water solvent was extracted with EA (50 mL x 3). The combined organic layers were dried over anhydrous Na_2SO_4, filtered, and concentrated under reduced pressure. The resulting residue was chromatographed over silica gel (3−8% MtOH in DCM) to give *N*-(6-(4-isopropyl-4*H*-1,2,4-triazol-3-yl)pyridin-2-yl)-4-(1-methyl-1*H*-pyrazol-4-yl)-1*H*-indole-2-carboxamide (**16**) (50 mg, 0.12 mmol, yield: 51%) as a white solid. mp 235−237 °C. ^{1}H NMR (400 MHz, DMSO-d_6) δ 12.00 (s, 1H), 10.78 (d, J = 7.1 Hz, 1H), 8.89 (s, 1H), 8.27 (s, 1H), 8.22 (d, J = 8.3 Hz, 1H), 8.10−8.00 (m, 2H), 7.96 (s, 1H), 7.80 (d, J = 7.6 Hz, 1H), 7.39−7.33 (m, 1H), 7.29−7.20 (m, 2H), 5.62−5.50 (m, 1H), 3.95 (s, 3H), 1.46 (d, J = 6.7 Hz, 6H). ^{13}C NMR (100 MHz, DMSO-d_6) δ 160.60, 151.92, 150.80, 146.63, 143.49, 139.90, 138.28, 137.65, 131.19, 129.25, 126.87, 125.08, 124.54, 121.40, 119.85, 117.81, 115.97, 110.96, 105.95, 48.35, 40.50, 23.64. HRMS-EI m/z [M + H]$^+$ calcd for $C_{23}H_{23}N_8O^+$: 427.1989, found: 427.1990. HPLC analysis: retention time = 4.046 min, 97.48%.

***N*-(6-(4-isopropyl-4*H*-1,2,4-triazol-3-yl)pyridin-2-yl)-5-(1*H*-pyrazol-4-yl)-1*H*-indole-2-carboxamide (17)** Compound **17** was prepared from 5-bromo-1*H*-indole-2-carboxylic acid **17-a** (142 mg, 0.59 mmol), key intermediate **8-d** (120 mg, 0.59 mmol) and 4-(4,4,5,5-tetramethyl-1,3,2- dioxaborolane-2-yl)-1*H*-pyrazole (115 mg, 0.59 mmol) according to a similar procedure described for the synthesis of compound **16**. White solid, 80 mg, yield: 33%. mp 295−297 °C. ^{1}H NMR (300 MHz, DMSO-d_6) δ 12.89 (s, 1H), 12.06 (s, 1H), 10.83 (s, 1H), 8.89 (s, 1H), 8.22 (d, J = 8.0 Hz, 1H), 8.04 (t, J = 7.9 Hz, 3H), 7.90 (s, 1H), 7.85 (d, J = 7.3 Hz, 1H), 7.57−7.43 (m, 3H), 5.81−5.66 (m, 1H), 1.47 (d, J = 6.7 Hz, 6H). ^{13}C NMR (100 MHz, DMSO-d_6) δ 160.62, 151.74, 150.60, 146.43, 143.63, 140.00, 136.46, 131.44, 127.89, 125.54, 123.58, 122.58, 119.74, 118.05, 115.84, 113.35, 106.08, 48.45, 23.59. HRMS-EI m/z [M + H]$^+$ calcd for $C_{22}H_{21}N_8O^+$: 413.1833, found: 413.1836. HPLC analysis: retention time = 3.389 min, 96.31%.

***N*-(6-(4-isopropyl-4*H*-1,2,4-triazol-3-yl)pyridin-2-yl)-6-(1*H*-pyrazol-4-yl)-1H-indole-2-carboxamide (21)** Compound **21** was prepared from 6-bromo-1*H*-indole-2-carboxylic acid **21-a** (165 mg,

0.69 mmol), key intermediate **8-d** (140 mg, 0.69 mmol) and 4-(4,4,5,5-tetramethyl-1,3,2- dioxaborolane-2-yl)-1*H*-pyrazole (134 mg, 0.69 mmol) according to a similar procedure described for the synthesis of compound **16**. White solid, 99 mg, yield: 35%. mp 159–161 °C. ^{1}H NMR (300 MHz, DMSO-d_6) δ: 12.92 (s, 1H), 11.88 (s, 1H), 10.66 (s, 1H), 8.89 (s, 1H), 8.23 (d, J = 8.2 Hz, 1H), 8.04 (t, J = 8.0 Hz, 2H), 7.85 (d, J = 7.6 Hz, 1H), 7.68 (d, J = 8.3 Hz, 1H), 7.62 (s, 1H), 7.54 (s, 1H), 7.38 (d, J = 8.3 Hz, 1H), 5.72–5.53 (m, 1H), 1.47 (d, J = 6.6 Hz, 6H). ^{13}C NMR (100 MHz, DMSO-d_6) δ 160.53, 151.85, 150.52, 146.67, 143.66, 139.88, 138.36, 131.18, 129.80, 125.88, 122.80, 122.51, 119.57, 115.65, 108.48, 106.60, 48.37, 23.70. HRMS-EI *m/z* [M + H]$^+$ calcd for $C_{22}H_{21}N_8O^+$: 413.1833, found: 413.1834. HPLC analysis: retention time = 3.465 min, 97.54%.

6-(1-(1-ethoxyethyl)-1*H*-pyrazol-4-yl)-*N*-(6-(4-isopropyl-4*H*-1,2,4-triazol-3-yl)pyridin-2-yl)-1*H*-indole-2-carboxamide (22) Compound **22** was prepared from 6-bromo-1*H*-indole-2-carboxylic acid **22-a** (188 mg, 0.79 mmol), key intermediate **8-d** (160 mg, 0.79 mmol) and 1-(1-ethoxyethyl)-4-(4,4,5,5-tetramethyl-1,3,2-dioxaborolan-2-yl)-1*H*-pyrazole (210 mg, 0.79 mmol) according to a similar procedure described for the synthesis of compound **16**. White solid, 130 mg, yield: 34%. mp 230–232 °C .^{1}H NMR (400 MHz, DMSO-d_6) δ 11.97 (s, 1H), 10.70 (s, 1H), 8.89 (s, 1H), 8.39 (s, 1H), 8.23 (d, J = 8.3 Hz, 1H), 8.04 (t, J = 8.0 Hz, 1H), 7.94 (s, 1H), 7.85 (d, J = 7.6 Hz, 1H), 7.69 (q, J = 6.0 Hz, 1H), 7.63 (s, 1H), 7.54 (s, 1H), 7.39 (dd, J = 8.3, 1.2 Hz, 1H), 5.79–5.66 (m, 1H), 5.58 (q, J = 5.9 Hz, 1H), 3.55–3.41 (m, 1H), 3.28–3.20 (m, 1H), 1.65 (d, J = 6.0 Hz, 3H), 1.47 (d, J = 6.8 Hz, 6H), 1.06 (t, J = 7.0 Hz, 3H). ^{13}C NMR (100 MHz, DMSO-d_6) δ 160.58, 151.91, 150.55, 146.69, 143.63, 139.85, 138.35, 136.71, 131.46, 129.18, 126.13, 125.34, 123.71, 122.86, 119.36, 115.70, 108.62, 106.66, 86.87, 63.51, 48.39, 23.69, 21.63, 15.20. HRMS-EI *m/z* [M + H]$^+$ calcd for $C_{26}H_{29}N_8O_2^+$: 485.2408, found: 485.2408. HPLC analysis: retention time = 4.616 min, 96.72%.

***N*-(6-(4-isopropyl-4*H*-1,2,4-triazol-3-yl)pyridin-2-yl)-6-(1-(tetrahydro-2*H*-pyran-4-yl)-1*H*-pyrazol-4-yl)-1*H*-indole-2-carboxamide (23)** Compound **23** was prepared from 6-bromo-1*H*-indole-2-carboxylic acid **23-a** (141 mg, 0.59 mmol), key intermediate **8-d** (120 mg, 0.59 mmol) and 1-(tetrahydro-2*H*-pyran-4-yl)-4-(4,4,5,5-tetramethyl-1,3,2-dioxaborolan-2-yl)- 1*H*-pyrazole (164 mg, 0.59 mmol) according to a similar procedure described for the synthesis of compound **16**. White solid, 79 mg, yield: 27%. mp 269–272 °C. ^{1}H NMR (400 MHz, DMSO-d_6) δ 11.87 (s, 1H), 10.64 (s, 1H), 8.90 (s, 1H), 8.27 (s, 1H), 8.23 (d, J = 8.1 Hz, 1H), 8.04 (t, J = 8.0 Hz, 1H), 7.89 (s, 1H), 7.85 (d, J = 7.6 Hz, 1H), 7.69 (d, J = 8.4 Hz, 1H), 7.60 (s, 1H), 7.55–7.52 (m, 1H), 7.36 (dd, J = 8.4, 1.3 Hz, 1H), 5.75–5.65 (m, 1H), 4.48–4.36 (m, 1H), 4.02–3.96 (m, 2H), 3.49–3.42 (m, 2H), 2.05–1.97 (m, 4H), 1.47 (d, J = 6.7 Hz, 6H). ^{13}C NMR (100 MHz, DMSO-d_6) δ 160.62, 151.87, 150.59, 146.69, 143.60, 139.89, 138.36, 136.23, 131.22, 129.57, 126.01, 125.37, 122.92, 119.40, 115.64, 108.38, 106.41, 66.42, 57.80, 48.36, 33.43, 23.66. HRMS-EI *m/z* [M + H]$^+$ calcd for $C_{27}H_{29}N_8O_2^+$: 497.2408, found: 497.2408. HPLC analysis: retention time = 3.932 min, 96.98%.

***N*-(6-(4-isopropyl-4*H*-1,2,4-triazol-3-yl)pyridin-2-yl)-6-(pyridin-3-yl)-1*H*-indole-2-carboxamide (24)** Compound **24** was prepared from 6-bromo-1*H*-indole-2-carboxylic acid **24-a** (153 mg, 0.64 mmol), key intermediate **8-d** (130 mg, 0.64 mmol) and 3-(4,4,5,5-tetramethyl-1,3,2- dioxaborolan-2-yl)pyridine (131 mg, 0.64 mmol) according to a similar procedure described for the synthesis of compound **16**. White solid, 78 mg, yield: 29%. mp 280–283 °C. ^{1}H NMR (300 MHz, DMSO-d_6) δ 12.07 (s, 1H), 10.74 (s, 1H), 8.91 (d, J = 11.9 Hz, 2H), 8.59 (d, J = 4.3 Hz, 1H), 8.24 (d, J = 8.1 Hz, 1H), 8.13 (d, J = 8.0 Hz, 1H), 8.05 (t, J = 7.9 Hz, 1H), 7.86 (dd, J = 8.0, 2.3 Hz, 2H), 7.76 (s, 1H), 7.64–7.60 (m, 1H), 7.54 (dd, J = 7.9, 4.9 Hz, 1H), 7.49–7.43 (m, 1H), 5.78–5.65 (m, 1H), 1.48 (d, J = 6.7 Hz, 6H). ^{13}C NMR (100 MHz, DMSO-d_6) δ 160.47, 151.78, 150.50, 148.57, 148.26, 146.73, 143.64, 139.93, 138.15, 137.03, 134.72, 133.78, 132.30, 127.25, 124.40, 123.26, 120.11, 119.65, 115.70, 111.09, 106.12, 48.34, 23.71. HRMS-EI *m/z* [M + H]$^+$ calcd for $C_{24}H_{22}N_7O^+$: 424.1880, found: 424.1882. HPLC analysis: retention time = 4.597 min, 98.75%.

***N*-(6-(4-isopropyl-4*H*-1,2,4-triazol-3-yl)pyridin-2-yl)-7-(1*H*-pyrazol-4-yl)-1*H*-indole-2-carboxamide (27)** Compound **27** was prepared from 7-bromo-1*H*-indole-2-carboxylic acid **27-a** (177 mg, 0.74 mmol), key intermediate **8-d** (150 mg, 0.74 mmol) and 4-(4,4,5,5-tetramethyl-1,3,2-dioxa borolan-2-yl)-1*H*-pyrazole (143 mg, 0.74 mmol) according to a similar procedure described for the synthesis of compound **16**. White solid, 94 mg, yield: 31%. mp 170–173 °C. ^{1}H NMR (300 MHz, DMSO-d_6) δ: 13.12 (s, 1H), 11.04 (s, 1H), 10.93 (s, 1H), 8.89 (s, 1H), 8.27 (d, J = 11.1 Hz, 1H), 8.04 (t, J = 7.8 Hz, 1H), 7.81 (d, J = 6.9 Hz, 1H), 7.61 (d, J = 8.1 Hz, 1H), 7.49 (s, 1H),7.41 (d, J = 7.2 Hz, 1H), 7.15 (s, 1H), 7.13 (t, J = 5.7 Hz, 1H), 6.85 (s, 1H), 5.40 (s, 1H), 1.45 (d, J = 5.4 Hz, 6H). ^{13}C NMR (100 MHz, DMSO-d_6) δ 160.20, 151.94, 150.64, 146.64, 143.53, 139.97, 134.90, 132.26, 128.22, 123.59, 121.29, 120.48, 119.82, 118.92, 117.92, 115.70, 108.77, 48.35, 23.65. HRMS-EI *m/z* [M + H]$^+$ calcd for $C_{22}H_{21}N_8O^+$: 413.1833, found: 413.1830. HPLC analysis: retention time = 4.040 min, 95.24%.

***N*-(6-(4-isopropyl-4*H*-1,2,4-triazol-3-yl)pyridin-2-yl)-7-(pyridin-4-yl)-1*H*-indole-2-carboxamide (28)** compound **28** was prepared from 7-bromo-1*H*-indole-2-carboxylic acid **28-a** (159 mg, 0.66 mmol), key intermediate **8-d** (134 mg, 0.66 mmol) and 4-(4,4,5,5-tetramethyl-1,3,2-dioxa borolan-2-yl)pyridine (135 mg, 0.66 mmol) according to a similar procedure described for the synthesis of compound **16**. White solid, 100 mg, yield: 36%, mp 278–280 °C. ^{1}H NMR (300 MHz, DMSO-d_6) δ 11.58 (s, 1H), 10.84 (s, 1H), 8.90 (s, 1H), 8.73 (s, 2H), 8.25 (d, J = 8.6 Hz, 1H), 8.06 (d, J = 7.7 Hz, 1H), 7.82 (d, J = 7.4 Hz, 2H), 7.72 (s, 2H), 7.59 (s, 1H), 7.39 (d, J = 6.9 Hz, 1H), 7.28 (d, J = 7.6 Hz, 1H), 5.57 (s, 1H), 1.46 (d, J = 6.2 Hz, 6H). ^{13}C NMR (100 MHz, DMSO-d_6) δ 160.07, 151.85, 150.59, 150.55, 150.52, 146.67, 146.08, 143.54, 140.04, 134.78, 132.74, 128.50, 125.38, 124.30, 123.98, 121.35, 119.88, 115.62, 108.28, 48.33, 23.65. HRMS-EI *m/z* [M + H]$^+$ calcd for $C_{24}H_{22}N_7O^+$: 424.1880, found: 424.1880. HPLC analysis: retention time = 5.000 min, 95.04%.

***N*-(6-(4-isopropyl-4*H*-1,2,4-triazol-3-yl)pyridin-2-yl)-7-(thiophen-3-yl)-1*H*-indole-2-carboxamide (29)** Compound **29** was prepared from 7-bromo-1*H*-indole-2-carboxylic acid **29-a** (165 mg, 0.69 mmol), key intermediate **8-d** (140 mg, 0.69 mmol) and 4,4,5,5-tetramethyl-2-(thiophen-3- yl)-1,3,2-dioxaborolane (145 mg, 0.69 mmol) according to a similar procedure described for the synthesis of compound **16**. White solid, 91 mg, yield: 31%. mp 178–181 °C. ^{1}H NMR (300 MHz, DMSO-d_6) δ 11.13 (s, 1H), 10.90 (s, 1H), 8.89 (s, 1H), 8.26 (d, J = 7.8 Hz, 1H), 8.05 (t, J = 8.0 Hz, 1H), 7.98 (dd, J = 2.8, 1.3 Hz, 1H), 7.82 (d, J = 7.0 Hz, 1H), 7.76 (dd, J = 5.0, 2.9 Hz, 1H), 7.70 (d, J = 7.8 Hz, 1H), 7.59–7.52 (m, 2H), 7.41 (dd, J = 7.2, 0.9 Hz, 1H), 7.24–7.15 (m, 1H), 5.58–5.52 (m, 1H), 1.46 (d, J = 6.7 Hz, 6H). ^{13}C NMR (100 MHz, DMSO-d_6) δ 160.11, 151.89, 150.65, 146.68, 143.53, 140.00, 138.88, 134.95, 132.35, 128.39, 128.36, 127.18, 124.64, 123.51, 121.85, 121.64, 121.28, 119.88, 115.61, 108.53, 48.33, 23.66. HRMS-EI *m/z* [M + H]$^+$ calcd for $C_{23}H_{21}N_6OS^+$: 429.1492, found: 429.1492. HPLC analysis: retention time = 7.333 min, 96.70%.

(*R*)-*N*-(6-(4-(1-hydroxypropan-2-yl)-4*H*-1,2,4-triazol-3-yl)pyridin-2-yl)-1*H*-indole-2-carboxamide (18) Step A: Compound **18-a** was prepared from compound **8-c** (500 mg, 1.90 mmol) and (*R*)-2-aminopropan-1-ol (712 mg, 9.5 mmol, 5.0 eq) according to a similar procedure described for the synthesis of compound **8** (step C). White solid, 255 mg, yield: 61%. ^{1}H NMR (300 MHz, $CDCl_3$) δ 8.36 (s, 1H), 7.54 (t, J = 8.1 Hz, 1H), 7.42 (d, J = 7.4 Hz, 1H), 6.57 (d, J = 8.2 Hz, 1H), 5.32–5.21 (m, 1H), 4.68 (s, 2H), 4.01 (d, J = 11.4 Hz, 1H), 3.86–3.40 (m, 2H), 1.52 (d, J = 6.8 Hz, 3H). MS (ESI) [M + H]$^+$:

220.1.

Step B: To a solution of compound **18-a** (200 mg, 0.57 mmol) in DME (10 mL) was added DIPEA (147 mg, 1.14 mmol, 2.0 eq) and tert-butyldimethylsilyl chloride (103 mg, 0.68 mmol, 1.2 eq), the mixture was stirred for 2 h at rt and the reaction was monitored by TLC. Upon completion, the reaction solution was concentrated under reduced pressure. The residue was partitioned between saturated aqueous $NaHCO_3$ (50 mL) and EA (50 mL). The organic layer was separated and washed with brine (50 mL), dried over Na_2SO_4, filtered, and concentrated under reduced pressure. The resulting residue was chromatographed over silica gel (10–35% EA in PE) to give (*R*)-6-(4-(1-((tert-butyldimethylsilyl)oxy)propan-2-yl)-4*H*-1,2,4-triazol-3-yl)pyridin-2-amine (**18-b**) (160 mg, 0.48 mmol, yield: 85%) as a white solid. ^{1}H NMR (300 MHz, $CDCl_3$) δ 8.43 (s, 1H), 7.59 (d, J = 3.3 Hz, 1H), 7.28 (d, J = 5.3 Hz, 1H), 6.58 (dd, J = 7.1, 1.9 Hz, 1H), 5.68–5.59 (m, 2H), 4.59 (s, 2H), 3.96 (s, 1H), 1.55 (d, J = 7.0 Hz, 3H), 0.96–0.90 (m, 6H), 0.87 (s, 9H). MS (ESI) $[M + H]^+$: 334.2.

Step C: Compound **18-c** was prepared from 1*H*-indole-2-carboxylic acid (193 mg, 1.20 mmol) and (*R*)-6-(4-(1-((tert-butyldimethylsilyl)oxy)propan-2-yl)-4*H*-1,2,4-triazol-3-yl)pyridin-2-amine **18-b** (400 mg, 1.20 mmol) according to a similar procedure described for the synthesis of compound **8** (step D). White solid, 359 mg, yield: 63%. ^{1}H NMR (300 MHz, DMSO-d_6) δ 11.89 (s, 1H), 10.65 (s, 1H), 8.80 (s, 1H), 8.21 (dd, J = 8.3, 0.6 Hz, 1H), 8.03 (t, J = 8.0 Hz, 1H), 7.84 (dd, J = 7.6, 0.3 Hz, 1H), 7.71 (d, J = 7.9 Hz, 1H), 7.55 (d, J = 1.5 Hz, 1H), 7.49 (d, J = 8.1 Hz, 1H), 7.32–7.23 (m, 1H), 7.15–7.04 (m, 1H), 5.65–5.57 (m, 1H), 3.69–3.59 (m, 2H), 1.48 (d, J = 6.9 Hz, 3H), 0.90–0.86 (m, 6H), 0.83 (s, 9H). MS (ESI) $[M + H]^+$: 477.2.

Step D: To a solution of compound **18-c** (200 mg, 0.42 mmol) in THF (10 mL) was added TBAF (220 mg, 0.84 mmol, 2.0 eq). The resulting mixture was stirred for 2 h at rt, the reaction was monitored by TLC. Upon completion, and the solvent was removed under reduced pressure. The residue was diluted with water (100 mL) and the water solvent was extracted with EA (100 mL x 3). The combined organic layers were dried over anhydrous Na_2SO_4, filtered, and concentrated under reduced pressure. The resulting residue was chromatographed over silica gel (20–40% EA in PE) to give (*R*)-*N*-(6-(4-(1-hydroxypropan-2-yl)-4*H*-1,2,4-triazol-3-yl)pyridin- 2-yl)-1*H*-indole-2- carboxamide (**18**) (100 mg, 0.28 mmol, yield: 66%) as a white solid. mp 255–257 °C. ^{1}H NMR (300 MHz, DMSO-d_6) δ 11.89 (s, 1H), 10.65 (s, 1H), 8.80 (s, 1H), 8.21 (d, J = 8.3 Hz, 1H), 8.03 (t, J = 8.0 Hz, 1H), 7.84 (d, J = 7.6 Hz, 1H), 7.71 (d, J = 7.9 Hz, 1H), 7.56 (d, J = 1.5 Hz, 1H), 7.49 (d, J = 8.2 Hz, 1H), 7.26 (t, J = 7.6 Hz, 1H), 7.09 (t, J = 7.5 Hz, 1H), 5.61 (q, J = 5.5 Hz, 1H), 4.99 (t, J = 5.4 Hz, 1H), 3.64 (d, J = 5.9 Hz, 2H), 1.49 (s, 3H). ^{13}C NMR (100 MHz, DMSO-d_6) δ 160.70, 151.70, 151.08, 146.84, 144.22, 139.88, 137.64, 131.17, 127.38, 124.77, 122.46, 120.62, 119.79, 115.58, 112.99, 106.04, 65.03, 53.79, 18.02. HRMS-EI *m/z* $[M + H]^+$ calcd for $C_{19}H_{19}N_6O_2^+$: 363.1564, found: 363.1567. HPLC analysis: retention time = 3.730 min, 96.04%.

7-acetamido-*N*-(6-(4-isopropyl-4*H*-1,2,4-triazol-3-yl)pyridin-2-yl)-1*H*-indole-2-carboxamide (25) Step A: To a solution of 2-nitrophenylhydrazine hydrochloride **25-a** (1.00 g, 5.27 mmol) in EtOH (20 mL) was added ethyl pyruvate (731 mg, 6.3 mmol, 1.2 eq) and the mixture was stirred at rt for 12 h, the reaction was monitored by TLC. Upon completion, the resulting mixture was concentrated under reduced pressure to give ethyl (*E*)-2-(2-(2-nitrophenyl)hydrazono)propanoate (**25-b**) (1.20 g, 4.80 mmol, yield: 91%) as a yellow solid, which was used for further reactions without purification. ^{1}H NMR (400 MHz, DMSO-d_6) δ 10.27 (s, 1H), 8.08 (t, J = 2.2 Hz, 1H), 7.78–7.70 (m, 1H), 7.68–7.63 (m, 1H), 7.56 (t, J = 8.1 Hz, 1H), 4.22 (q, J = 7.1 Hz, 2H), 2.09 (d, J = 10.6 Hz, 3H), 1.28 (t, J = 7.1 Hz, 3H). MS (ESI) $[M + H]^+$: 252.1.

Step B: A solution of **25-b** (1.20 g, 4.78 mmol) in polyphosphoric acid (20 mL) was heated at 80 °C for 3 h, the reaction was monitored by TLC. Upon completion, the mixture was then allowed to cooled to rt. The reaction was diluted with water, followed by carefully acidified to pH 8 by slow addition of saturated aqueous NaOH solution, the resulting aqueous mixture was extracted with EA (100 mL × 3). The mixture was washed with H_2O (100 mL), brine (100 mL), dried over Na_2SO_4, filtered, and concentrated under reduced pressure. The residue was chromatographed over silica gel (0–30% EA in PE) to give ethyl 7-nitro-1*H*-indole-2-carboxylate (**25-c**) (794 mg, 3.39 mmol, yield: 71%) as a yellow solid. ^{1}H NMR (300 MHz, DMSO-d_6) δ: 11.38 (s, 1H), 8.29 (dd, J = 8.0, 2.3 Hz, 1H), 8.23 (dd, J = 7.7 Hz, 2.4 Hz, 1H), 7.47(t, J = 2.0 Hz, 1H), 7.43–7.35 (m, 1H), 4.39 (q, J = 7.1 Hz, 2H), 1.37 (t, J = 11.6 Hz, 3H). MS (ESI) $[M + H]^+$: 235.1.

Step C: To a solution of **25-c** (794 mg, 3.39 mmol) in EtOH/H_2O (12 mL, 2 mL) was added Fe (957 mg, 17.0 mmol, 5 eq) followed by NH_4Cl (1.10 g, 20.0 mmol, 6.0 eq). The mixture was stirred at 80 °C for 4 h, the reaction was monitored by TLC. Upon completion, the reaction mixture was filtered through Celite. The filter cake was washed with 10% MeOH in DCM (30 mL), and the biphasic mother liquor was separated. The aqueous phase was further extracted with DCM (50 mL × 3), and the combined organic extracts were washed with H_2O (50 mL), brine (50 mL), dried over Na_2SO_4, filtered, and concentrated under reduced pressure. The residue was chromatographed over silica gel (0–5% MeOH in DCM) to give ethyl 7-amino-1*H*-indole-2- carboxylate (**25-d**) (394 mg, 1.93 mmol, 57%) as a white solid. ^{1}H NMR (300 MHz, DMSO-d_6) δ: 11.42 (s, 1H), 7.02 (d, J = 2.1 Hz, 1H), 6.85–6.76 (m, 2H), 6.42 (dd, J = 7.0, 1.2 Hz, 1H), 5.41 (s, 2H), 4.34 (q, J = 7.1 Hz, 2H), 1.34 (t, J = 7.1 Hz, 3H). MS (ESI) $[M + H]^+$: 205.1.

Step D: To a solution of **25-d** (200 mg, 0.98 mmol) in DCM (10 mL) was added DIPEA (253 mg, 1.96 mmol, 2.0 eq) followed by acetyl chloride (115 mg, 1.47 mmol, 1.5 eq). The mixture was stirred at rt for 3 h, the reaction was monitored by TLC. Upon completion, the mixture was concentrated under reduced pressure and then poured into H_2O (50 mL) and extracted with EA (50 mL × 3). The combined organic extracts were washed with H_2O (50 mL), brine (50 mL), dried over Na_2SO_4, filtered, and concentrated under reduced pressure. The residue was chromatographed over silica gel (0–5% MeOH in DCM) to give ethyl 7-acetamido-1*H*-indole-2-carboxylate (**25-e**) (150 mg, 0.61 mmol, yield: 62%) as a white solid. ^{1}H NMR (300 MHz, DMSO-d_6) δ: 11.65 (s, 1H), 9.80 (s, 1H), 7.93 (s, 1H), 7.39 (d, J = 7.8 Hz, 1H), 7.25–6.93 (m, 2H), 2.38 (d, J = 6.9 Hz, 3H), 2.19 (d, J = 13.7 Hz, 3H), 1.49–1.25 (m, 3H). MS (ESI) $[M + H]^+$: 247.1.

Step E: To a solution of **25-e** (150 mg, 0.61 mmol) in THF (10 mL) was added a solution of NaOH (49 mg, 1.22 mmol, 2.0 eq) in H_2O (2 mL). The mixture was stirred at rt for 3 h, the reaction was monitored by TLC. Upon completion, the resulting reaction was then extracted with EA (30 mL × 2). The aqueous phase was subsequently neutralized to pH 2 with 2 N aqueous HCl and then extracted with EA (30 mL × 3), and the combined organic extracts were concentrated under reduced pressure. The residue was chromatographed over silica gel (0–20% MeOH in DCM) to give 7-acetamido-1*H*-indole-2-carboxylic acid (**25-f**) (100 mg, 0.46 mmol, yield: 75%) as a white solid. ^{1}H NMR (300 MHz, DMSO-d_6) δ: 12.07 (s, 1H), 11.65 (s, 1H), 9.80 (s, 1H), 7.93 (s, 1H), 7.39 (d, J = 7.8 Hz, 1H), 7.25–6.93 (m, 2H), 2.38 (d, J = 6.9 Hz, 3H). MS (ESI) $[M + H]^+$: 219.1.

Step F: Compound **25** was prepared from 7-acetamido-1*H*-indole-2-carboxylic acid **25-f** (161 mg, 0.73 mmol) and key intermediate **8-d** (150 mg, 0.73 mmol) according to a similar procedure described for the synthesis of compound **8** (step D). White solid, 114 mg, yield: 39%. mp 269–272 °C. ^{1}H NMR (300 MHz, DMSO-d_6) δ 11.82 (s, 1H), 10.80 (s, 1H), 9.94 (s, 1H), 8.89 (s, 1H), 8.22 (d,

$J = 8.2$ Hz, 1H), 8.05 (t, $J = 7.9$ Hz, 1H), 7.96 (d, $J = 7.5$ Hz, 1H), 7.86 (d, $J = 7.4$ Hz, 1H), 7.62 (s, 1H), 7.44 (d, $J = 7.8$ Hz, 1H), 7.05 (t, $J = 7.8$ Hz, 1H), 5.80–5.63 (m, 1H), 2.18 (s, 3H), 1.47 (d, $J = 6.5$ Hz, 6H). ^{13}C NMR (100 MHz, DMSO-d_6) δ 169.07, 160.55, 151.74, 150.52, 146.72, 143.62, 139.93, 130.88, 128.71, 128.69, 125.24, 120.96, 119.70, 117.73, 115.77, 114.80, 106.59, 48.35, 24.45, 23.69. HRMS-EI m/z $[M + H]^+$ calcd for $C_{21}H_{22}N_7O_2^+$: 404.1829, found: 404.1835. HPLC analysis: retention time = 3.703 min, 99.38%.

5.2. ASK1 kinase assay

ASK1 kinase activity of target compounds was measured using the Homogeneous Time Resolved Fluorescence (HTRF) assay kit (Cisbio, Catalog #62ST3PEB) with full-length recombinant human ASK1 (MAP3K5) (Carna, Catalog #07–107). The assay procedure is as follows: (1) Dilution series of test compounds were prepared in 100% DMSO and assay buffer (1 X Enzymatic, 5 mM $MgCl_2$, 1 mM DTT), and 2.0 μL of diluted compounds were dispensed to the individual wells of a white optiplate-384. (2) 4 μL of MAP3K5 (5 ng/μL) in assay buffer and 4 μL of STK-Substrate 3-biotin (5 μM)/ATP (250 μM) in assay buffer were added to the assay plates containing test compounds. (3) Assay plates were incubated for 2 h at rt and 5 μL of STK S3 Antibody-Eu (500 nM) in assay buffer was added. (4) The assay plates were incubated for an additional 1 h at rt and then read on an EnVision plate reader using a 340 nm excitation wavelength and 665 nm emission wavelength for fluorescence detection. The final amount of enzyme in the assay was 2 nM ASK1, the final concentration of STK-Substrate 3-biotin was 2 μM and the final concentration of DMSO was 2%. IC_{50} values were obtained using Prism 8.0 (GraphPad Software).

5.3. AP1-HEK293 cell assay

AP1-HEK293 cell activity of select compounds was measured using AP1 Reporter-HEK293 cells according to the manufacturer's instructions. Reagents: (1) Thaw Medium 1 (BPS Catalog #60187): MEM medium (Hyclone Catalog #SH30024.01) supplemented with 10% FBS (Life technologies Catalog #26140-079), 1% non-essential amino acids (Hyclone Catalog #SH30238.01), 1 mM Na-pyruvate (Hyclone Catalog #SH30239.01), 1% Penicillin/Streptomycin (Hyclone Catalog #SV30010.01). (2) Growth Medium 1B (BPS Catalog #79531): Thaw Medium 1 (BPS Catalog #60187) and 400 μg/mL of Geneticin (Life Technologies Catalog #11811031). (3) AP1 Reporter-HEK293 cells (BPS Catalog #60405). (4) Phorbol-12-Myristate-13-Acetate (PMA) (LC Laboratories Catalog #P-1680). (5) Assay medium: Opti-MEMI (Life Technologies Catalog #31985-062), 0.5% FBS, 1% nonessential amino acids, 1 mM Na pyruvate, and 1% Pen/Strep. (6) ONE-Step™ Luciferase Assay Reagent (BPS Catalog #60690). The assay procedure is as follows. (1) Harvest AP1 Reporter–HEK293 cells from culture in Growth Medium 1B and seed cells at a density of 35,000 cells per well into a white clear-bottom 96-well microplate in 100 μL of Thaw Medium 1. (2) Incubate the cells at 37 °C in a CO_2 incubator for overnight. (3) The next day, the compounds stock were diluted in assay medium. Carefully remove the medium from wells and add 90 μL of diluted compounds in assay medium to the wells. The final concentration of DMSO in assay medium can be up to 0.5%. Add 90 μL of assay medium with same concentration of DMSO without compound to compound control wells. Add 90 μL of assay medium with DMSO to cell-free control wells (for determining background luminescence). (4) Incubate the plate at 37 °C in a CO_2 incubator for 1 h (5) Add 10 μL of diluted PMA in assay medium to stimulated wells (final concentration of PMA was 10 nM). Final DMSO concentration should be 0.1%. Add 10 μL of assay medium with 0.1% DMSO to the unstimulated control wells (cells without inhibitor and PMA treatment for determining the basal activity). Add 10 μL of assay medium with 0.1% DMSO to cell-free control wells. (6) Incubate the plate at 37 °C in a CO_2 incubator for 6 h (7) Perform luciferase assay using the ONE-Step™ Luciferase Assay System following the protocol provided: Add 100 μL of ONE-Step™ Luciferase reagent per well and rock at rt for 15 min. Measuring luminescence using a luminometer. (8) Data Analysis: Obtain background-subtracted luminescence by subtracting average background luminescence (cell-free control wells) from luminescence reading of all wells.

5.4. Cell membrane permeability assay

The membrane permeability of compounds 6 and 19 was evaluated using MDRI-MDCKII cells by Sundia MediTech Co., Ltd (Shanghai, China). The assay procedure is as follows. (1) While 80–90% of cell culture bottle was adhered with cells, the cell culture medium was discarded. (2) The cell culture bottle was washed with 5 mL of 10 mM PBS buffer (37 °C) and then the PBS was discarded. (3) The adhered cells were dissolved with 5 mL of 0.05% Trypsin-EDTA, then 10 mL of cell culture medium (37 °C) was added to terminate reaction, centrifuged (900 rpm, 3 min). (4) Supernatant of cell culture medium was discarded and 10 mL of new cell culture medium (37 °C) was added to calculate. The cells were diluted to 2×10^5 cells/mL. (5) Cells were seeded into 24-multiwell Insert Systems with PET (polyethylene terephthalate) membranes (1 μm pore size and 0.3 cm^2 surface area) at an optimized density of 2×10^5 cells/ml in cell culture medium. (6) Before transport study, all the apical sides and basolateral sides were washed with 0.3 mL and 1 mL of PBS buffer (pH 7.4) for 30 min at 37 °C, in 5% CO_2 incubator. (7) MDRI-MDCKII cell monolayers were preincubated (at 37 °C, in 5% CO_2 incubator) in transport media, all the apical sides and basolateral sides were preincubated with 0.2 mL and 0.7 mL of the transport media with or without specific P-gp inhibitor cyclosporin A for 40 min (8) The test compounds were diluted with DMEM to the final incubation conc. of 10 μM, While the control compound was diluted by DMEM to the final incubation conc. of 3 μM. (9) For A to B directional transport, 0.2 mL of donor working solution with test articles or positive control was added to the A compartment and 0.7 mL of the transport media as receiver working solution then to the B compartment. For B to A directional transport, 0.7 mL of donor working solution with test articles or positive control was added to the B compartment and 0.2 mL of the transport media as receiver working solution then to the A compartment. The cells were incubated (37 °C, in 5% CO_2 incubator) for 90 min (10) 80 μL of samples were taken from both donor and receiver compartments into 96-well assay plates, which pre-added with 240 μL internal standard (IS) solution of acetonitrile each well, and centrifuged (5000 rpm, 10 min). (11) 80 μL of supernatant were taken into 96-well assay plates pre-added with 160 μL ultrapure water and then analyzed by LC-MS/MS.

5.5. In vivo rat pharmacokinetic study

The pharmacokinetic study of compound **19** was performed by Shanghai ChemPartner Co., Ltd. (Shanghai, China). The assay procedure is as follows. (1) 6 male SD rats were obtained from JH Laboratory Animal Co., Ltd. (Shanghai, China), Fasted 24 h, divided into two groups randomly (n = 3 per group). The first group SD rats by 1 mg/kg dose intravenous to give solution of compound **19** in 10% DMAC +10% (30% Solutol HS 15 in water) + 80% Saline. The second group SD rats by 10 mg/kg dose lavage to give suspension of compound **19** in 0.5% CMC and 0.5% Tween 80 in water. (2) Took blank blood before giving medicine, took about 150 μL of venous blood at different time points after the treatment of compound **19** in Eppendorf tube with heparin, centrifuged, took plasma about

50 μL, −70 °C saved for testing. The point time of blood collection, iv injection: 0.083 h, 0.25 h, 0.5 h, 1 h, 2 h, 4 h, 8 h and 24 h oral administration: 0.25 h, 0.5 h, 1 h, 2 h, 4 h, 8 h and 24 h (3) Processing and determination of the plasma samples: An aliquot of 50 μL sample was added with 200 μL IS (Dexamethasone, 300 ng/mL in ACN). The mixture was vortexed for 10 min at 750 rpm and centrifuged at 6000 rpm for 10 min. An aliquot of 0.5 μL supernatant was injected for LC−MS/MS analysis. (4) The calculation method of pharmacokinetic parameters: the blood drug concentration-time data to the DAS 2.1.1 program using the statistical method to calculate pharmacokinetic parameters.

5.6. Docking study

The X-ray crystal structures of ASK1 (PDB codes 3VW6 and 5VIO) were downloaded from the Protein Data Bank (www.rcsb.org). Protein crystal structure 5VIO was prepared using Protein Preparation Wizard and Grid generation in Schrodinger suite. Compounds **6**, **9** and **11** were prepared using Ligand Preparation module in Schrodinger. Then, compounds **6**, **9** and **11** were docked into ASK1 (5VIO) by Glide Docking in Schrodinger. The images files were generated using Pymol software.

5.7. DSS-induced mouse UC model and compounds treatment

Male ICR mice (18−22 g, 6−8 weeks old) were purchased from Comparative Medical Center of Yangzhou University (Yangzhou, China). Before starting the experiments, the mice were housed in a constant room, with a maintained temperature (22 ± 2 °C), humidity (55 ± 5%), and lighting (12 h light/dark cycle) for 5 days to acclimatize the lab environment. All animals were allowed free access to water and food. Animal experiments were organized and conducted in accordance with the guidelines of the National Institutes of Health Guide and Care of Laboratory Animals. The methods were approved by the Animal Care and Use Committee of China Pharmaceutical University. ICR mice were randomly divided into four groups (n = 6 per group): control group, model group, compound **19** group and compound **6** group. The model group, compound **19** group and compound **6** group mice were given 3% DSS (w/v) orally in drinking water to induce UC and the control group mice were received distilled water for 7 days. The drinking water were changed every two days. Compounds **19** and **6** were administered (po, qd) at a dose of 25 mg/kg during the DSS treatment for 7 days, meanwhile, control group and model group mice were treated with vehicle. The mice were observed and the changes in body weight, stool consistency and rectal bleeding were recorded once a day. All experimental mice were sacrificed at the end of experiment, the colons were harvested and colon length was measured. The colon tissues were collected immediately, fixed in 4% formaldehyde and preserved for H&E staining analysis; the remaining colon tissues were stored at −80 °C for further examination.

5.8. Disease activity index (DAI) scores and body weight changes

DAI scores and body weight changes were calculated according to the following standards. Body weight loss: 0 = none, 1 = 1−5%, 2 = 5−10%, 3 = 1015%, 4 = over 15%; stool consistency: 0 = normal, 1 = loose stools, 2 = diarrhea; blood in stool: 0 = normal, 1 = fecal occult blood, 2 = gross bleeding. Mean of the above three factors was calculated as DAI scores. Body weight changes (%) were calculated on the basis of body weight loss [44,45].

5.9. Hematoxylin-eosin (H&E) staining

The colon tissues were fixed in 4% formaldehyde and embedded in paraffin for sectioning. Then the colon tissues were cut into 4-μM thick sections and stained with hematoxylin and eosin. Histopathological changes were observed using a computer-assisted light microscope (CX23, Olympus, Japan).

5.10. Western blotting

The colon tissues were weighed and homogenized in ice-cold RIPA buffer. The lysates were centrifuged and the supernatants were collected. Bicinchoninic acid (BCA) protein assay kit was used for quantification of protein content. The protein samples were separated using sodium salt-polyacrylamide gel electrophoresis (SDS-PAGE) and then transferred to PVDF membrane. After blocking with 5% Bovine Serum Albumin at rt for 2 h, the membrane was incubated with primary antibodies overnight at 4 °C. Then the membrane was washed three times with TBST buffer, incubated with the horseradish peroxidase (HRP)-conjugated anti-rabbit antibody for 2 h at rt, then displayed using an ECL detection kit and quantified by gel analysis software. Primary antibodies: anti-ASK1 (Catalog #AF6477), anti-MKK3/6 (Catalog #AF6327), anti-MKK4/7 (Catalog #AF4734), anti-p38 (Catalog #AF6456), anti-JNK (Catalog #AF6318), anti-p-ASK1 (Catalog #AF8096), anti-*p*-MKK3/6 (Catalog #AF3805), anti-*p*-MKK4/7 (Catalog #AF4434), anti-p-p38 (Catalog #AF4001), anti-*p*-JNK (Catalog #AF3318) antibodies were purchased from Affinity Biosciences, Inc. (Jiangsu, China), and anti-GAPDH (Catalog #bs-0755R) antibody was obtained from Bioss Antibodies, Inc. (Beijing, China).

5.11. Enzyme-linked immunosorbent assay (ELISA)

The homogenates of mouse colon tissues were centrifuged and the supernatants were collected. The expression levels of inflammatory cytokines (IL-1β, IL-6 and TNF-α) were measured using ELISA kits following the manufacturer's instructions. Mouse IL-1β ELISA kit (Catalog #EMC001b.48), IL-6 ELISA kit (Catalog #K4144-100) and TNF-α ELISA kit (Catalog #ADI-900-047) were provided by Neobioscience Technology Co., Ltd. (Shanghai, China).

Declaration of competing interest

The authors declare that they have no known competing financial interests or personal relationships that could have appeared to influence the work reported in this paper.

Acknowledgment

This work was financially supported by the National Natural Science Foundation of China (Program Nos. 81973182 and 81673301) and "Double First-Class" University Project from China Pharmaceutical University (Program No. CPU2018GF02). We thank Prof. Cheng-Ming Chiang of UT Southwestern Medical Center for revising this manuscript.

Abbreviations

ASK1	apoptosis signal-regulating kinase 1
MAPK	mitogen-activated protein kinase
DSS	dextran sulfate sodium
UC	ulcerative colitis
DAI	disease activity index
IBD	inflammatory bowel disease
CRC	colorectal cancer

ALS	amyotrophic lateral sclerosis
CIA	collagen-induced arthritis
NASH	nonalcoholic steatohepatitis
NaF	sodium fluoride
TNBS	2,4,6-trinitrobenzene sulfonic acid
DIPEA	*N,N*-Diisopropylethylamine

Appendix A. Supplementary data

Supplementary data to this article can be found online at https://doi.org/10.1016/j.ejmech.2020.113114.

References

[1] C.A. Lamb, N.A. Kennedy, T. Raine, P.A. Hendy, P.J. Smith, J.K. Limdi, B.H. Hayee, M.E. Lomer, G. C Parkes, C. Selinger, K.J. Barrett, R.J. Davies, C. Bennett, S. Gittens, M.G. Dunlop, O. Faiz, A. Fraser, V. Garrick, P.D. Johnston, M. Parkes, J. Sanderson, H. Terry, D.R. Gaya, T.H. Iqbal, S.A. Taylor, M. Smith, M. Brookes, R. Hansen, A.B. Hawthorne, British society of gastroenterology consensus guidelines on the management of inflammatory bowel disease in adults, Gut 68 (2019) 1–106.

[2] Y. Chen, P. Zhang, W.R. Chen, G. Chen, Ferroptosis mediated DSS-induced ulcerative colitis associated with Nrf2/HO-1 signaling pathway, Immunol. Lett. 225 (2020) 9–15.

[3] A. Rocchi, E.I. Benchimol, C.N. Bernstein, A. Bitton, B. Feagan, R. Panaccione, K.W. Glasgow, A. Fernandes, S. Ghosh, Inflammatory bowel disease: a Canadian burden of illness review, Chin. J. Gastroenterol. Hepatol. 26 (2016) 811–817.

[4] S.C. Ng, H.Y. Shi, N. Hamidi, F.E. Underwood, W. Tang, E.I. Benchimol, J.C. Wu, F.K. Chan, J.J. Sung, G. Kaplan, The worldwide incidence and prevalence of inflammatory bowel disease in the 21st century: a systematic review of population-based studies, Gastroenterology 152 (2017) 970–971.

[5] M. Fumery, S. Singh, P.S. Dulai, C. Gower-Rousseau, L. Peyrin-Biroulet, W.J. Sandborn, Natural history of adult ulcerative colitis in population-based cohorts: a systematic review, Clin. Gastroenterol. Hepatol. 16 (2018) 343–356.

[6] A.N. Ananthakrishnan, C.N. Bernstein, D. Iliopoulos, A. Macpherson, M.F. Neurath, R.A. Raja Ali, S.R. Vavricka, C. Fiocchi, Environmental triggers in IBD: a review of progress and evidence, Nat. Rev. Gastroenterol. Hepatol. 15 (2018) 39–49.

[7] S.B. Kang, H.S. Yoo, S.H. Jeon, C.W. Song, N.R. Lee, N.J. Kim, J.K. Lee, K.S. Inn, Identification of 3′,4′,5′-trihydroxyflavone as an mammalian target of rapamycin inhibitor and its suppressive effects on dextran sulfate sodium-induced ulcerative colitis, Int. Immunopharm. 84 (2020) 106524.

[8] Y.Z. Zhang, Y.Y. Li, Inflammatory bowel disease: pathogenesis, World J. Gastroenterol. 20 (2014) 91–99.

[9] P.L. Beck, J.L. Wallace, Cytokines in inflammatory bowel disease, Mediat. Inflamm. 6 (1997) 95–103.

[10] M.F. Neurath, Cytokines in inflammatory bowel disease, Nat. Rev. Immunol. 14 (2014) 329–342.

[11] M. Friedrich, M. Pohin, F. Powrie, Cytokine Networks in the pathophysiology of inflammatory bowel disease, Immunity 50 (2019) 992–1006.

[12] J.K. Yamamoto-Furusho, Inflammatory bowel disease therapy: blockade of cytokines and cytokine signaling pathways, Curr. Opin. Gastroenterol. 34 (2018) 187–193.

[13] T. Sairenji, K.L. Collins, D.V. Evans, An update on inflammatory bowel disease, PrimaryCare 44 (2017) 673–692.

[14] C.N. Bernstein, Treatment of IBD: where we are and where we are going, Am. J. Gastroenterol. 110 (2015) 114–126.

[15] O. Hauso, T.C. Martinsen, H. Waldum, 5-Aminosalicylic acid, a specific drug for ulcerative colitis, Scand. J. Gastroenterol. 50 (2015) 933–941.

[16] H. Ichijo, E. Nishida, K. Irie, P. Dijke, M. Saitoh, T. Moriguchi, M. Takagi, K. Matsumoto, K. Miyazono, Y. Gotoh, Induction of apoptosis by ASK1, a mammalian MAPKKK that activates SAPK/JNK and p38 signaling pathways, Science 275 (1997) 90–94.

[17] S. Schuster, A.E. Feldstein, NASH: novel therapeutic strategies targeting ASK1 in NASH, Nat. Rev. Gastroenterol. Hepatol. 14 (2017) 329–330.

[18] A. Matsuzawa, H. Nishitoh, K. Tobiume, K. Takeda, H. Ichijo, Physiological roles of ASK1-mediated signal transduction in oxidative stress-and endoplasmic reticulum stress-induced apoptosis: advanced findings from ASK1 knockout mice, Antioxidants Redox Signal. 4 (2002) 415–425.

[19] C. Sakauchi, H. Wakatsuki, H. Ichijo, K. Hattori, Pleiotropic properties of ASK1, Biochim. Biophys. Acta 1861 (2017) 3030–3038.

[20] Y. Kawarazaki, H. Ichijo, I. Naguro, Apoptosis signal-regulating kinase 1 as a therapeutic target, Expert Opin. Ther. Targets 18 (2014) 651–664.

[21] T. Fujisawa, Therapeutic application of apoptosis signal-regulating kinase 1 inhibitors, Adv Biol Regul 66 (2017) 85–90.

[22] T. Fujisawa, M. Takahashi, Y. Tsukamoto, N. Yamaguchi, M. Nakoji, M. Endo, H. Kodaira, Y. Hayashi, H. Nishitoh, I. Naguro, K. Homma, H. Ichijo, The ASK1-specific inhibitors K811 and K812 prolong survival in a mouse model of amyotrophic lateral sclerosis, Hum. Mol. Genet. 25 (2016) 245–253.

[23] Y. Hayakawa, Y. Hirata, K. Sakitani, H. Nakagawa, W. Nakata, H. Kinoshita, R. Takahashi, K. Takeda, H. Ichijo, S. Maeda, K. Koike, Apoptosis signal-regulating kinase 1 inhibitor as a potent therapeutic drug for the treatment of gastric cancer, Canc. Sci. 103 (2012) 2181–2185.

[24] M. Lanier, J. Pickens, S.V. Bigi, E.L. Bradshaw-Pierce, A. Chambers, Z.S. Cheruvallath, D. Dougan, J. Ermolieff, T. Gibson, P. Halkowycz, A. Hirokawa, A. Ivetac, J. Miura, E. Nunez, M. Sabat, J. Tyhonas, H.X. Wang, X. Wang, S. Swann, Structure-based design of ASK1 inhibitors as potential agents for heart failure, ACS Med. Chem. Lett. 8 (2017) 316–320.

[25] J.T. Liles, B.K. Corkey, G.T. Notte, G.R. Budas, E.B. Lansdon, F. Hinojosa-Kirschenbaum, S.S. Badal, M. Lee, B.E. Schultz, S. Wise, S. Pendem, M. Graupe, L. Castonguay, K.A. Koch, M.H. Wong, G.A. Papalia, D.M. French, T. Sullivan, E.G. Huntzicker, F.Y. Ma, D.J. Nikolic-Paterson, T. Altuhaifi, H.C. Yang, A.B. Fogo, D.G. Breckenridge, ASK1 contributes to fibrosis and dysfunction in models of kidney disease, J. Clin. Invest. 128 (2018) 4485–4500.

[26] G. Nygaard, J.A. Di Paolo, D. Hammaker, D.L. Boyle, G. Budas, G.T. Notte, I. Mikaelian, V. Barry, G.S. Firestein, Regulation and function of apoptosis signal-regulating kinase 1 in rheumatoid arthritis, Biochem. Pharmacol. 151 (2018) 282–290.

[27] Y. Terao, H. Suzuki, M. Yoshikawa, H. Yashiro, S. Takekawa, Y. Fujitani, K. Okada, Y. Inoue, Y. Yamamoto, H. Nakagawa, S.H. Yao, T. Kawamoto, O. Uchikawa, Design and biological evaluation of imidazo[1,2-a]pyridines as novel and potent ASK1 inhibitors, Bioorg, Med. Chem. Lett. 22 (2012) 7326–7329.

[28] S.A. Harrison, V.W. Wong, T. Okanoue, N. Bzowej, R. Vuppalanchi, Z. Younes, A. Kohli, S. Sarin, S.H. Caldwell, N. Alkhouri, M.L. Shiffman, M. Camargo, G. Li, K. Kersey, C. Jia, Y. Zhu, C.S. Djedjos, G.M. Subramanian, R.P. Myers, N. Gunn, A. Sheikh, Q.M. Anstee, Romero-Gomez, M. Trauner, Z. Goodman, E.J. Lawitz, Z. Younossi, Selonsertib for patients with bridging fibrosis or compensated cirrhosis due to NASH: results from randomized phase III STELLAR trials, J. Hepatol. 73 (2020) 26–39.

[29] L. Chen, P. Kuang, H. Liu, Q. Wei, H. Cui, J. Fang, Z.C. Zuo, J.L. Deng, Y.L. Li, X. Wang, L. Zhao, Sodium fluoride (NaF) induces inflammatory responses via activating MAPKs/NF-kappaB signaling pathway and reducing anti-inflammatory cytokine expression in the mouse Liver, Biol. Trace Elem. Res. 189 (2019) 157–171.

[30] H.Z. Li, X. Han, K.Y. Zuo, L. Li, J.T. Liu, X.H. Yuan, Y.C. Shen, M.L. Shao, D.X. Pang, Y.H. Chu, B.H. Zhao, MiR-23b promotes cutaneous wound healing through inhibition of the inflammatory responses by targeting ASK1, Acta Biochim. Biophys. Sin. 50 (2018) 1104–1113.

[31] A. Matsuzawa, K. Saegusa, T. Noguchi, C. Sadamitsu, H. Nishitoh, S. Nagai, S. Koyasu, K. Matsumoto, K. Takeda, H. Ichijo, ROS-dependent activation of the TRAF6-ASK1-p38 pathway is selectively required for TLR4-mediated innate immunity, Nat. Immunol. 6 (2005) 587–592.

[32] P. Gurung, S. Banskota, N. Katila, J. Gautam, T.M. Kadayat, D.Y. Choi, E.S. Lee, T.C. Jeong, J.A. Kim, Ameliorating effect of TI-1-162, a hydroxyindenone derivative, against TNBS-induced rat colitis is mediated through suppression of RIP/ASK-1/MAPK signaling, Eur. J. Pharmacol. 827 (2018) 94–102.

[33] G. Samak, K.K. Chaudhry, R. Gangwar, D. Narayanan, J.H. Jaggar, R. Rao, Calcium/ASK1/MKK7/JNK2/c-Src signalling cascade mediates disruption of intestinal epithelial tight junctions by dextran sulfate sodium, Biochem. J. 465 (2015) 503–515.

[34] N. Baregamian, J. Song, C.E. Bailey, J. Papaconstantinou, B.M. Evers, D.H. Chung, Tumor necrosis factor-α and apoptosis signal-regulating kinase 1 control reactive oxygen species release, mitochondrial autophagy and c-Jun N-terminal kinase/p38 phosphorylation during necrotizing enterocolitis, Oxidative Med. Cell. Longev. 2 (2009) 297–306.

[35] M. Okamoto, N. Saito, H. Kojima, T. Okabe, K. Takeda, H. Ichijo, T. Furuya, T. Nagano, Identification of novel ASK1 inhibitors using virtual screening, Bioorg, Med. Chem. 19 (2011) 486–489.

[36] A. Monastyrskyi, S. Bayle, V. Quereda, W. Grant, M. Cameron, D. Duckett, W. Roush, Discovery of 2-arylquinazoline derivatives as a new class of ASK1 inhibitors, Bioorg. Med. Chem. Lett 28 (2017) 400–404.

[37] S.A. Starosyla, G.P. Volynets, S.S. Lukashov, O.B. Gorbatiuk, A.G. Golub, V.G. Bdzhola, S.M. Yarmoluk, Identification of apoptosis signal-regulating kinase 1 (ASK1) inhibitors among the derivatives of benzothiazol-2-yl-3-hydroxy-5-phenyl-1,5-dihydro-pyrrol-2-one, Bioorg. Med. Chem. 23 (2015) 2489–2497.

[38] T.S. Gibson, B. Johnson, A. Fanjul, P. Halkowycz, D.R. Dougan, D. Cole, S. Steven, Structure-based drug design of novel ASK1 inhibitors using an integrated lead optimization strategy, Bioorg. Med. Chem. Lett 27 (2017) 1709–1713.

[39] G.P. Volynets, V.G. Bdzhola, A.G. Golub, A.R. Synyugin, M.A. Chekanov, O.P. Kukharenko, S.M. Yarmoluk, Rational design of apoptosis signal-regulating kinase 1 inhibitors: discovering novel structural scaffold, Eur. J. Med. Chem. 61 (2012) 104–115.

[40] G.P. Volynets, M.O. Chekanov, A.R. Synyugin, A.G. Golub, O.P. Kukharenko, V.G. Bdzhola, S.M. Yarmoluk, Identification of 3H-naphtho[1,2,3-de]quinoline-2,7-diones as inhibitors of apoptosis signal-regulating kinase 1 (ASK1), J. Med. Chem. 54 (2011) 2680–2686.

[41] M.K. Himmelbauer, Z.L. Xin, J.H. Jones, I. Enyedy, K. King, D.J. Marcotte, P. Murugan, J.C. Santoro, T. Hesson, K. Spilker, J.L. Johnson, M.J. Luzzio, R. Gilfillan, F.G. de Turiso, Rational design and optimization of a novel class of macrocyclic apoptosis signal-regulating kinase 1 inhibitors, J. Med. Chem. 62 (2019) 10740–10756.

[42] F. Lovering, P. Morgan, C. Allais, A. Aulabaugh, J. Brodfuehrer, J. Chang, J. Coe,

W.D. Ding, H. Dowty, M. Fleming, R. Frisbie, J. Guzova, D. Hepworth, J. Jasti, S. Kortum, R. Kurumbail, S. Mohan, N. Papaioannou, J.W. Strohbach, F. Vincent, K. Lee, C.W. Zapf, Rational approach to highly potent and selective apoptosis signal-regulating kinase 1 (ASK1) inhibitors, Eur. J. Med. Chem. 145 (2018) 606–621.

[43] R. Brys, K. Gibson, T. Poljak, S. Van Der Plas, D. Amantini, Discovery and development of ASK1 inhibitors, Prog. Med. Chem. 59 (2020) 101–179.

[44] F. Xie, H. Zhang, C. Zheng, X.F. Shen, Costunolide improved dextran sulfate sodium-induced acute ulcerative colitis in mice through NF-kappaB, STAT1/3, and Akt signaling pathways, Int. Immunopharm. 84 (2020) 106567.

[45] M. Murano, K. Maemura, I. Hirata, K. Toshina, T. Nishikawa, N. Hamamoto, S. Sasaki, O. Saitoh, K. Katsu, Therapeutic effect of intracolonically administered nuclear factor kappa B (p65) antisense oligonucleotide on mouse dextran sulphate sodium (DSS)-induced colitis, Clin. Exp. Immunol. 120 (2000) 51–58.